THESIS

EVALUATION OF POWER-ASSIST HYDRAULIC AND ELECTRIC HYBRIDS FOR MEDIUM- AND HEAVY-DUTY VEHICLE APPLICATIONS

Submitted by

Justin Taylor Wagner

Department of Mechanical Engineering

In partial fulfillment of the requirements

For the Degree of Master of Science

Colorado State University

Fort Collins, Colorado

Summer 2014

Master's Committee:

Advisor: Thomas H. Bradley

Todd M. Bandhauer
Ronald M. Sega

ABSTRACT

EVALUATION OF POWER-ASSIST HYDRAULIC AND ELECTRIC HYBRIDS FOR MEDIUM- AND HEAVY-DUTY VEHICLE APPLICATIONS

Under pressure from rising fuel costs, emissions constraints, and new government regulations on medium- and heavy-duty vehicles, hybrid technologies for these classes of vehicles are becoming more prevalent. A variety of technologies have been proposed to meet these requirements including power-assist hybrid electric and hybrid hydraulic systems. Although there has been great discussion about the benefits surrounding each of the technologies individually, no direct comparisons are available on the basis of economics and fuel economy. This study focuses on comparing these power-assist technologies on these bases as well as determines the ability of these technologies to fulfill the newly adopted fuel economy regulations.

In order to accomplish this goal, three computational models of vehicle dynamics, thermal behavior and fuel economy were created and validated to simulate the conventional vehicle and hydraulic and electric hybrids. These models were simulated over the Heavy-Duty Urban Dynamometer Driving Schedule, the HTUF Class 4 Parcel Delivery Cycle, and the Orange County Bus cycle. These drive cycles were chosen on their ability to characterize the variety of operating conditions observed in medium- and heavy-duty vehicles. Using these models, cross technology comparisons were constructed comparing commercially available systems, systems with a fixed mass, and systems with a fixed incremental cost.

The results of the commercially available systems showed that the Azure Dynamics HEV provided greater fuel economy improvement than the Lightning Hybrids HHV for drive cycle kinetic intensities less than 3.19 $miles^{-1}$. Although this system showed a cost of fuel savings over the HHV, it was seen that the incremental cost of the HEV exceeded the cost of fuel savings over the HHV. The fixed mass comparison case, which compared vehicles with equal cargo carrying utility, showed similar results to that of the commercially available case. Although the increase in incremental cost for the varying HEV systems designed for the fixed mass case correlated to an improvement in fuel savings, the cost associated with the systems surpassed the savings seen. Lastly, the fixed cost case provided results which were also similar to the commercially available case. Due to the fixed system cost, it was seen that for these systems, the fuel economy benefits and associated cost showed the greatest benefits for the HEV.

This study concluded that given the evaluation, the HEV was the only power-assist hybrid technology which could fulfill the regulated fuel economy improvement of 15%. Although the HEV was the only technology which could fulfill the requirements, the HHV showed an improvement upwards of 7% greater than the HEV for the Orange County Bus Drive Cycle.

ACKNOWLEDGEMENTS

I would like to thank several people for their support in the process of my working towards my M.S. in Mechanical Engineering. I would like to begin by thanking my advisor, Dr. Thomas Bradley, for providing me with opportunities to work on several projects while I have been one of his graduate students. I would also like to thank Dr. Ronald Sega and Dr. Todd Bandhauer for being on my thesis committee.

I would like to thank my parents for their love and support. I would also like to thank my brother, Nick Wagner, for pushing me to get to where I am now and for providing me with opportunities to prove myself.

I would also like to thank several key members of the lab group. I would like to thank Jacob Renquist, Ben Geller, and Jake Bucher for their assistance in completing this thesis.

Lastly, I would like to thank Lightning Hybrids for the opportunity which they provided me through funding this project as well as the necessary guidance to complete it. Specifically, I would like to thank Brian Johnston for providing me with the guidance and knowledge necessary to perform the analysis within this thesis.

TABLE OF CONTENTS

LIST OF TABLES

LIST OF FIGURES

INTRODUCTION

Until recently, medium- and heavy-duty vehicles were not required to uphold emissions and fuel economy standards mandated by the United States' government. In 2011, these classes of vehicles composed 4.48% of all of the vehicles on the roads in the United States yet consumed 26.8% of the 12.68 million barrels of petroleum daily [1], [2]. In an attempt to lower the fuel consumed from these vehicles, the new Environmental Protection Agency (EPA) and National Highway and Traffic Safety Administration (NHTSA) regulations mandate a fuel economy improvement of 15% by model year 2018 [3].

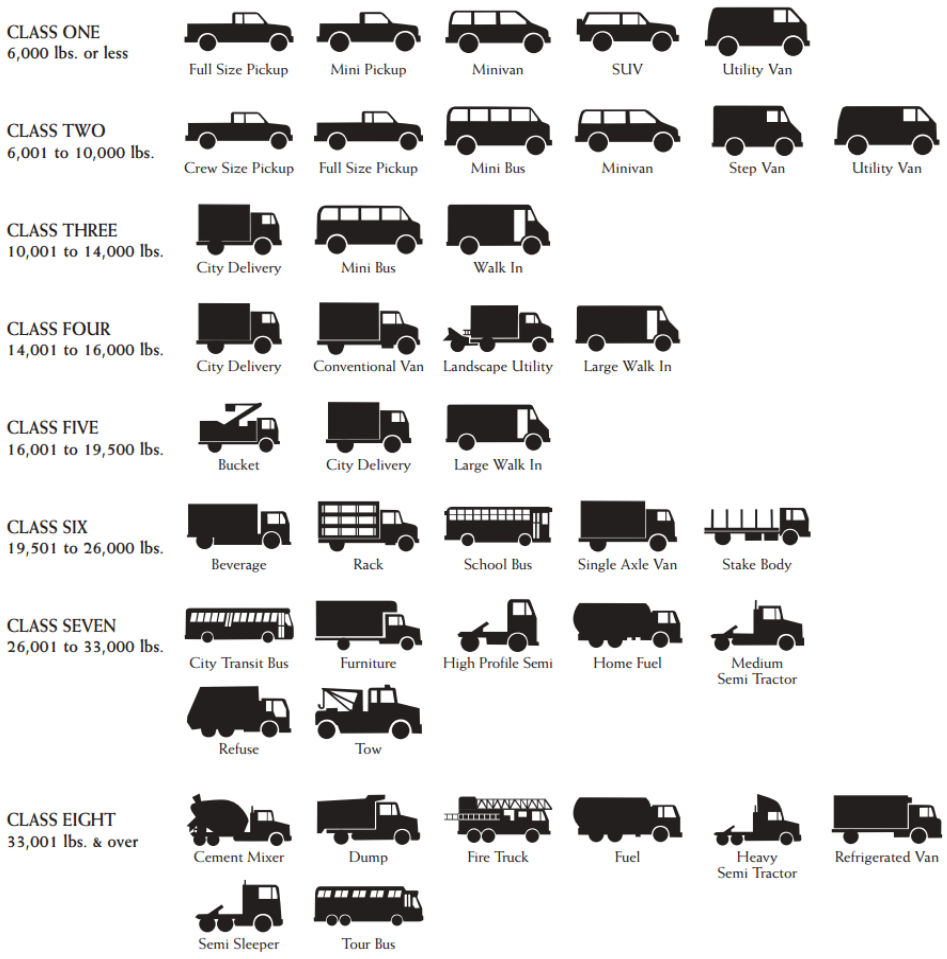

Figure 1: Vehicle Weight Classifications and Vehicle Examples for Each [4]

As defined by the EPA, medium- and heavy duty vehicles are characterized by the gross vehicle weight (GVW). In Figure 1 above, light-duty passenger vehicles are defined as classes 1 and 2a which have a GVW less than 8500lbs and include cars and light trucks. Medium-duty vehicles are defined as having a GVW between 8500lb and 14000lb and include large passenger trucks (GMC 3500, Ford F-350, etc.), delivery vans (Mercedes Sprinter, Ford Transit, etc.) and service vehicles. The heaviest of the vehicle classes is the heavy-duty vehicles, which include all automobiles with a GVW greater than 14000lb. Included in these vehicles are larger delivery vehicles, city buses, and combination tractor-trailers. The EPA and NHTSA regulations focus on all classes between Class 2b (8500 GVW) and Class 8 (>33001 GVW). Within these classes of vehicles, there are many fuel saving technologies currently on the market to assist in achieving the goals of these new regulations.

FUEL SAVING TECHNOLOGIES

The current state of the automobile market, there are many technologies which assist in making vehicles more fuel efficient. The potential of each of these technologies can be seen in Figure 2, below. Some technologies which have the potential to reduce fuel consumption include weight reduction, rolling resistance reduction, and aerodynamic drag reduction, more efficient transmission and drivetrain design, new engine technologies, and hybridization. The fuel consumption reduction available ranges from 0% to 35% for these technologies.

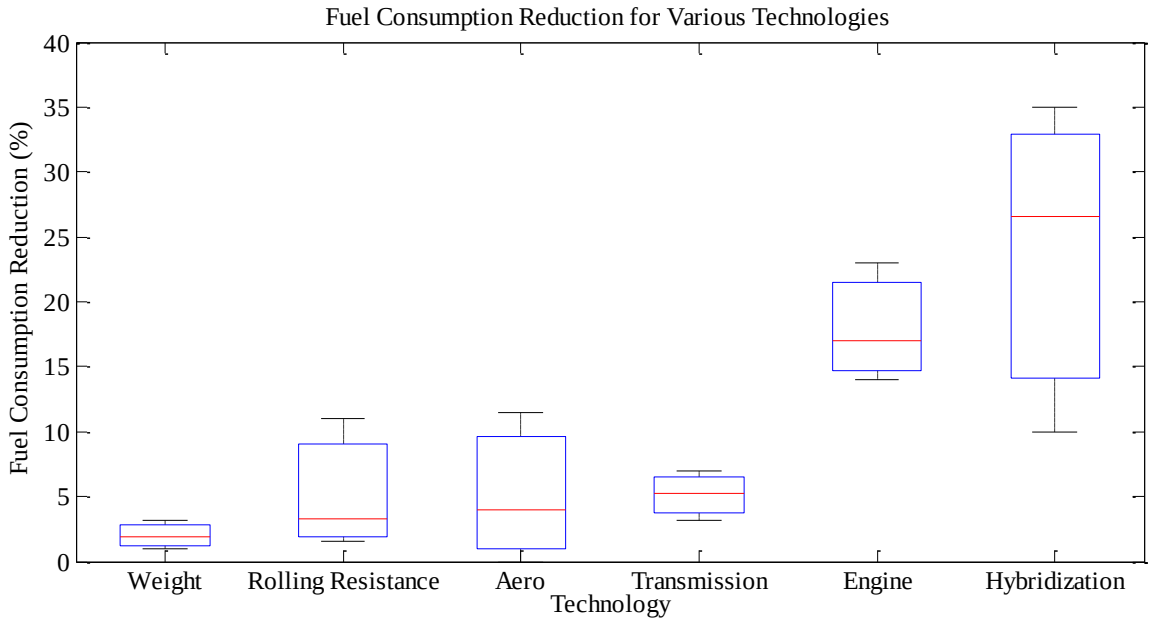

Figure 2: Fuel Consumption Reduction for Various Technologies [5]

According to the National Academies Study of 2010, the technology with the least potential for reducing fuel economy in heavy duty vehicles is weight reduction. In general, by reducing the overall empty weight of a vehicle, some fuel will be saved. Light-weighting methods include replacing wood components and other panels with lighter materials including aluminum and composites and reducing drivetrain component sizes. The potential of reducing vehicle weight as a method of reducing fuel consumption ranges between 1% and 4% depending on the vehicle class. Light-weighting reduces fuel economy through reducing the overall energy required for the vehicle operation. Another method of reducing the rolling resistance of the vehicle includes improving tire technology. The reduction of rolling resistance has the potential to reduce fuel consumption between 1.5% and 11%. The next most effective technology in reducing fuel consumption is the reduction of aerodynamic drag. Some of the devices which reduce aerodynamic drag include side skirts, end-cap fairings, gap fairings, step fairings and roof fairings. Examples of these devices can be seen in the figure below.

Figure 3: Examples of rolling resistance and drag reduction for trucks. (A) Low Rolling Resistance Tires, (B) Side Fairings, (C) Step Fairing, (D) End-Cap Fairing, (E) Roof Fairing, and (F) Gap Fairing [6].

The inclusion of these devices has the potential to reduce fuel consumption between 0% and 11.5%. Improvements to the transmission and drivetrain have the potential to reduce fuel consumption between 3.2% and 7%. Methods of engine improvements which have the potential to reduce fuel consumption include the addition of variable valve timing, reduction of engine friction, engine downsizing, and the reduction of accessory loads. Through these methods, fuel consumption can be reduced between 11.2% and 23%. The technology which has the potential for the greatest reduction in fuel economy is hybridization. These methods include the ability of recapturing some of the kinetic energy of the vehicle by assisting in braking, through the use of motors and storage systems. This recaptured energy can then be reapplied to the drivetrain by using the stored energy and applying it to the motors which add torque to the drivetrain. The potential of hybridization for medium- and heavy-duty vehicles in the reduction of fuel consumption varies between 10% and 40%.

VEHICLE HYBRIDIZATION

A hybrid vehicle is a vehicle with two or more energy sources. In this, hybrid vehicles are often composed of a combination of internal combustion engines (ICE) and power electronics or hydraulic systems. In order to save fuel, hybrid vehicle technologies use various mechanisms in order to reduce overall fuel consumption of the vehicle. Included in these mechanisms are: regenerative braking, engine downsizing, and the ability to operate the vehicle in most efficient

regions. Regenerative braking in hybrid vehicles is the ability to capture the vehicles kinetic energy though using a motor to apply braking torque. The application of braking torque causes the vehicle to slow, and it additionally recharges the hybrid energy storage device. This ability assists in reducing fuel economy through increasing the hybrid systems stored energy. With the inclusion of hybrid systems, vehicles can be designed with smaller engines since they have a secondary torque source. This coincides with a fuel consumption reduction since smaller engines typically burn fuel at a slower rate. The final method of reducing fuel consumption is in some systems the engine can be controlled to operate at its most efficient operating point. [7]

Hybrid vehicles are available in various architectures to fully utilize and implement the fuel saving mechanisms. Included in these architectures is the series, parallel, and power-split architectures. The series architecture provides the power necessary for the road load from the hybrid system and maintains the necessary hybrid energy through charging via the ICE. The series architecture provides the ability to decouple the ICE from the road load and allows the engine to be operated within its most efficient region. A parallel architecture provides two independent power flows to provide the necessary power for the road load. The first path is from the ICE through the transmission to the driveshaft and out to the wheels, and the second path is from the hybrid motor through the driveshaft and out to the wheels. This architecture allows for power to flow purely from the engine, purely from the hybrid system, or a combination of both. A power flow diagram for the parallel architecture can be seen in Figure 4, below. The last architecture which is prevalent in hybrid vehicles is the power-split architecture which is a provides the power flows available from both the ICE and the hybrid systems to the wheels as well as the ability to store expended energy from the ICE within the hybrid system [8].

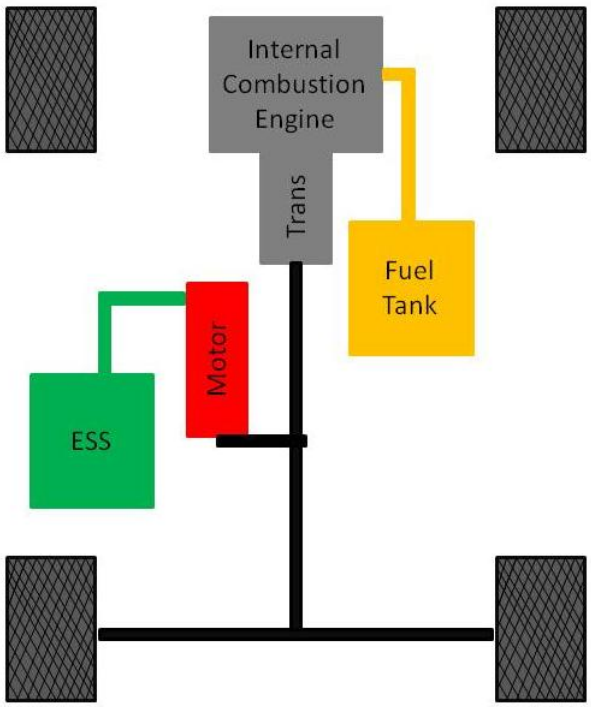

Figure 4: Parallel Hybrid Power Flow Diagram

In Figure 4 above, the overall powertrain configuration for a parallel hybrid can be seen. It can be seen that in addition to the traditional path of fuel (in yellow) to the internal combustion engine (gray), there is a hybrid path which is aft the transmission. Similar to the fuel tank, there is hybrid energy storage system (ESS), seen in green, and there is also a tractive hybrid motor (red). For the purposes of this study, the parallel electric and hydraulic hybrid architectures will be compared.

For parallel hybrids, there are many common methods for interpreting a drivers' throttle input. For this study, the throttle interpretation style referred to as torque addition, or power-assist, was utilized. The torque addition interpretation reads the drivers throttle command and applies equal throttle to both the ICE and the hybrid drivetrain. Due to the decrease in throttle position, this interpretation method can save fuel by decreasing the overall load upon the ICE.

ELECTRIC HYBRIDS

Electric hybridization provides a path of energy through the use of electrochemical devices and electric motors. These electrochemical devices, or batteries, can be used and charged in various ways: Charge Depletion, Charge Sustention, and Grid Charging. These methods are commonly used together to increase the range of the hybrid system. Charge depletion is a control mode where the vehicle begins its drive with above a specified minimum state of charge (SOC). While above this SOC, the controller relies primarily on the electric system to meet tractive loads and runs the engine at a minimum. As this process continues, the SOC decreases until it reaches the minimum SOC where the controller switches to a charge sustaining mode. In the charge sustaining mode, the vehicle relies heavily on the engine and uses the hybrid system to complement the engine and maintains a SOC close to the minimum SOC. The final charging method of electric hybrids is grid charging. Vehicles which have this ability are considered Plug-In Electric Vehicles. These vehicles, which not being operated, rely on the electricity grid to charge them. Milder hybrids operate primarily within the charge sustaining mode of operation. These vehicles are entirely independent of the electric grid and they maintain the minimum storage charge through regenerative braking.

Electric Energy Storage

In electric hybrids, energy is stored in electrochemical or electrostatic devices. The electrochemical devices, more commonly referred to as batteries, are composed of varying chemistries. Compounds which have been incorporated in battery hybrids include Lithium-Ion, Nickel Metal Hydride, and Lead Acid. Each of the battery chemistries have characteristics as can be seen in Table 1.

Table 1: Cell characteristics for Lead Acid, Lithium Ion, and Nickel Metal Hydride Batteries [9].

	Cell Voltage	Specific Energy
Lead Acid	2.4	35
Lithium Ion	4.0	250-400
Nickel Metal Hydride	1.2	50-80

From the battery cell characteristics listed above in Table 1, it can be seen that the battery chemistry causes variance in both the cell voltage and specific energy. When making battery packs for electric vehicles, the combination of cell voltage and specific energy come into play in designing the battery pack. Most recently, Lithium-Ion batteries have become the most common battery for vehicle hybridization [10].

Electric Motors

For use in electric hybrids, the primary motor technology incorporated is alternating current (AC) permanent magnet synchronous motors. In comparison to DC motors, the AC motors used in hybrid vehicles are fairly similar in cost; however the AC motors require the use of more complex controllers and power inverters. Although the overall cost of the AC motors (including the controller and inverter) is greater than a DC motor, the AC motors are more efficient and require less maintenance [11].

HYDRAULIC HYBRIDS

The second hybrid method which will be analyzed is the use of hydraulic systems. Hydraulic hybrids recover energy through the use of hydraulic pumps/motors and accumulators.

Hydraulic Pumps and Motors

For use in transportation, hydraulic hybrids offer two types of pumps, fixed and variable displacement. The variable displacement pump offers the ability to easily change the displacement and torque of the pump by changing the swash plate angle. The fixed displacement

pump offers a fixed fluid displacement and torque. Although the fixed displacement pump size determines the torque and fluid displacement, this can be varied through the use of valves. The use of valves, however, comes at the cost of efficiency. Hydraulic pumps and motors, however quite efficient at high pressures and speeds, have a significant loss in efficiency at lower speeds and pressures.

Hydraulic Energy Storage

Hydraulic hybridization stores energy through the use of accumulators. Most hydraulic accumulators for transportation use are composed of composites and are of two varieties, piston or bladder. Both accumulator technologies store energy through the compression of nitrogen gas through the movement of hydraulic fluid.

Piston accumulators separate the nitrogen gas and hydraulic fluid with a piston as can be seen in on the left side of Figure 5. As hydraulic fluid is pumped into a piston accumulator, the piston expands the volume of the fluid region, thus compressing the nitrogen gas in the opposite compartment. Bladder accumulators, as seen on the right in Figure 5, use hydraulic fluid to compress a neoprene bladder filled with nitrogen. When hydraulic fluid is pumped into a bladder accumulator, the nitrogen gas filled bladder is compressed by the increase in hydraulic fluid volume.

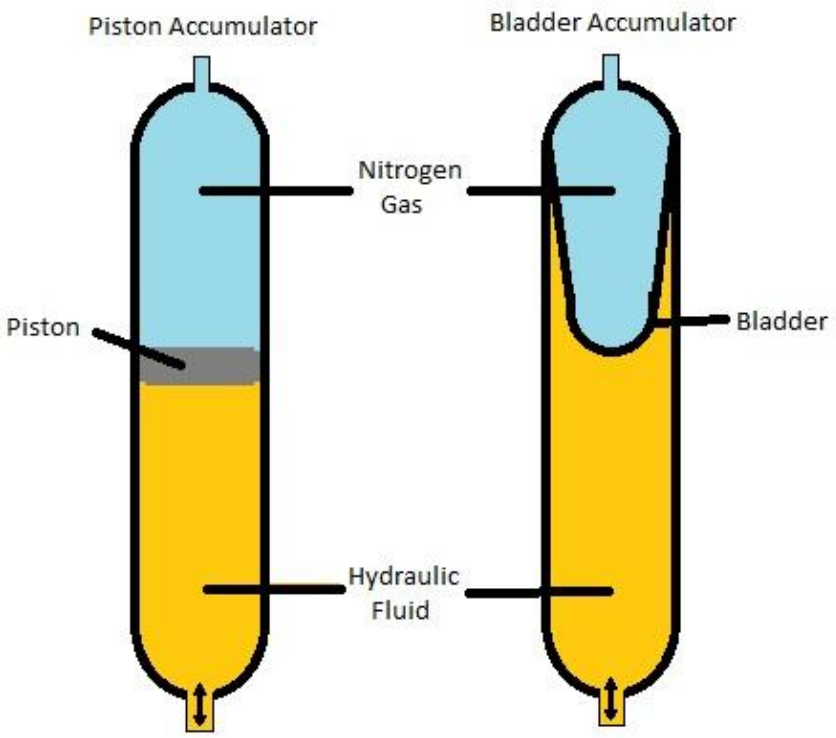

Figure 5: Overview of Piston (Left) and Bladder (Right) Type Hydraulic Accumulators

For hydraulics, the energy which is stored is a function of the pressure and volume stored within the accumulator. The following equation shows the relationship between the stored energy, the pressure, and the volume [12].

$$E = \frac{V_0 P_0^{\frac{1}{n}}}{n-1}\left(P_{max}^{\frac{n-1}{n}} - P_0^{\frac{n-1}{n}}\right) \quad (1)$$

As can be seen in Equation (1), the stored energy is a function of the precharge conditions, as described previously, and the instantaneous volume and pressure. The concept of precharging an accumulator is setting the minimum power through pressurizing the gas. The total energy which is stored within the accumulator is based upon this precharge pressure and the maximum pressure of the system as seen in the equation above. For the purpose of this study, the precharge pressure is set to 2500 psi.

RESEARCH QUESTION

This study is meant to answer a research question pertaining to the function and uses for hybrid technology on medium- and heavy-duty vehicles.

Although there are many studies which discuss the benefits of each hybrid technology individually, there are currently no studies which make a direct comparison of the two technologies on the basis of initial cost, life time fuel cost, and fuel economy [14], [15], [16], [17]. Given this lack of comparison, how do electric and hydraulic hybrid power-assist technologies compare on the basis of fuel economy, incremental cost, and fueling cost over drive cycles of varying kinetic intensity and under which conditions do these technologies fulfill the newly adopted EPA and NHTSA fuel economy regulations?

This research question is answered through the following procedure described below and in depth in the following chapters.

- Determine drive cycles characteristic of the operation of these classes of vehicles and create analytic models through which to simulate fuel economy results corresponding to each technology.
- Validate the analytic models through results from dynamometer testing for each of the technologies as well as validation standards for vehicle testing.
- Present results from simulations on the basis of commercially available systems, systems with a fixed cost, and systems with a fixed mass and evaluate these results to perform a comparison on the basis of incremental cost, life time fuel cost and fuel economy.

A discussion and conclusion of these results will further analyze and present the comparison of these technologies and their abilities to fulfill the fuel economy requirements.

VEHICLE MODELING

The Simulink models of these vehicles and hybrid technologies were created following the Rose-Hulman Institute of Technology Model-Based Systems Design lecture notes [18]. These lectures covered the design of the conventional vehicle as well as a series electric hybrid. In order to model the parallel electric and the hydraulic hybrids, several changes were made to these models and are discussed below.

DRIVE CYCLE SELECTION

In order to perform the simulations, it was decided that the drive cycles used would have to be characteristic of the driving conditions observed by medium- and heavy-duty vehicles. Each of the drive cycles chosen represented a different mode of operation for vehicles within medium- and heavy-duty classes. Included in these modes was parcel delivery (HTUF Class 4 Parcel Delivery Drive Schedule), city bus (Orange County Bus), urban driving (Heavy-Duty Vehicle Urban Dynamometer Driving Schedule).The time series plots of these drive cycles can be seen in Figure 6, below. In addition to the chosen drive cycles representing various modes of operation within the medium- and heavy-duty vehicle classes, the drive cycles vary in kinetic intensity.

According to the National Renewable Energy Laboratory (NREL), kinetic intensity is a value used to characterize drive cycles as a ratio of the characteristic acceleration to the aerodynamic speed. This ratio can be seen in the Equation (2), below.

$$ki = \frac{\tilde{a}}{{v_{aero}}^2} \tag{2}$$

The characteristic acceleration referred to by kinetic intensity is defined by NREL as the inertial work required to accelerate the vehicle or change the vehicle's altitude per unit of mass and per unit of distance. The dynamometer drive cycles do not incorporate an altitude profile

with the velocity profile, so the characteristic acceleration for all of the drive cycles in this study is a function only of the work required to accelerate the vehicle. The denominator of the kinetic intensity equation is the aerodynamic speed. NREL defines the aerodynamic speed as the ratio of the cubic speed to the average drive cycle speed. The following equation shows kinetic intensity as it is defined.

$$ki \cong \frac{\sum_{j=1}^{N-1} positive\left(\frac{1}{2}\cdot\left(v_{j+1}^2 - v_j^2\right)\right)}{\sum_{j=1}^{N-1}\overline{v_{j,J+1}^3}\cdot\Delta t_{j,j+1}} \quad (3)$$

The drive cycle with the lowest kinetic intensity is that of the Heavy-Duty Vehicle Urban Dynamometer Driving Schedule (HDV UDDS) which has a kinetic intensity of 0.68/mile. In increasing order, the next drive cycle, the HTUF Class 4 Parcel Delivery Driving Schedule (HTUF-4), has a kinetic intensity of 1.51/mile. The last drive cycle, which requires the greatest kinetic energy per mile, is the Orange County Bus drive cycle (OCBus). OCBus features a kinetic intensity of 3.6/mile [19].

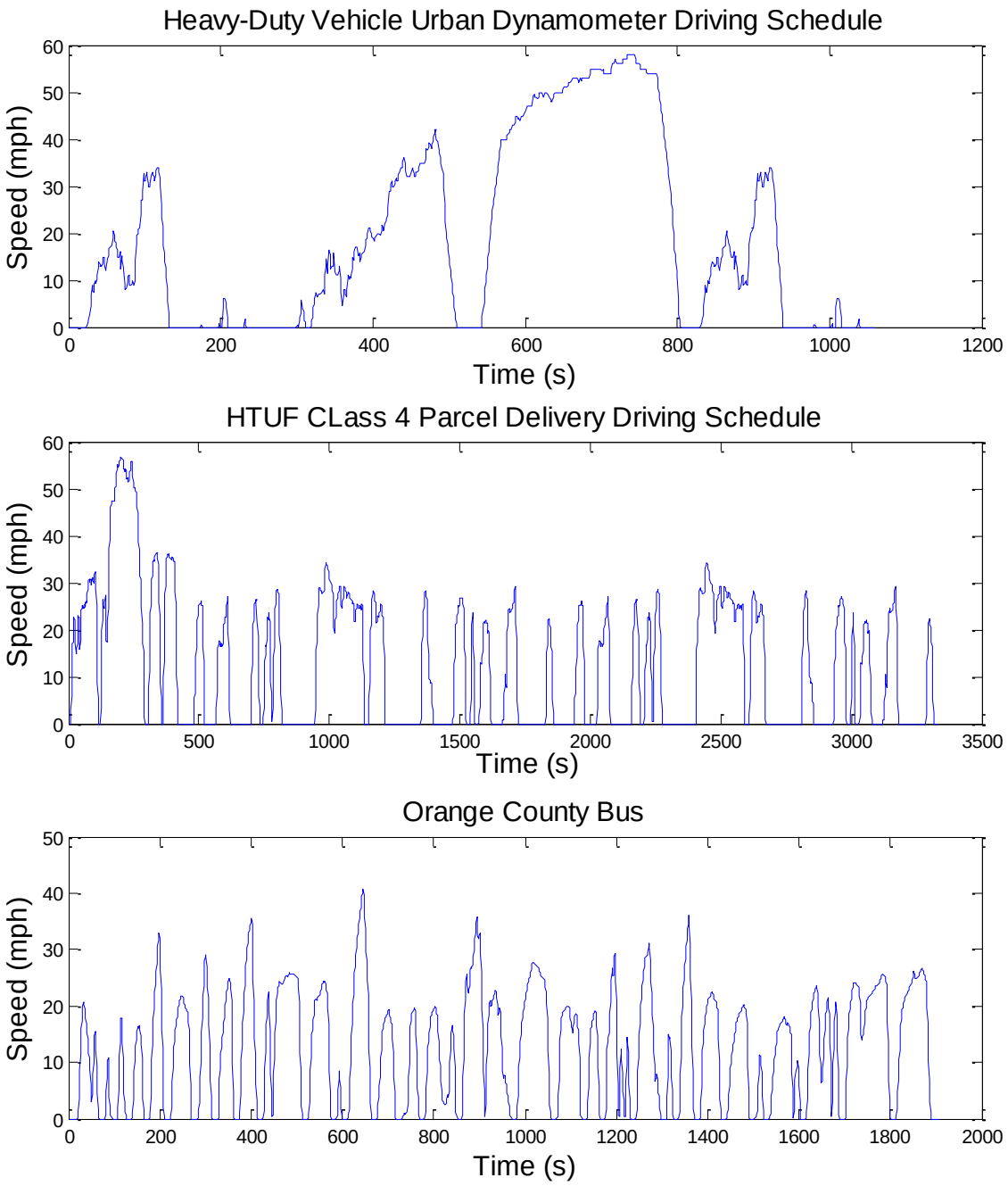

Figure 6: Heavy-Duty Vehicle Urban Dynamometer Driving Schedule (Top), HTUF Class 4 Parcel Delivery Driving Schedule (Middle), and Orange County Bus (Bottom) Drive Cycles

CONVENTIONAL VEHICLE MODEL

The conventional vehicle which was modeled was for a 2013 GMC Savana 3500 Cutaway Van. This vehicle chassis is used in several medium-duty applications such as shuttle buses, service trucks, and delivery vans.

Figure 7: GMC Savana 3500 Cutaway Van [20]

The Savana 3500 Cutaway is a medium-duty empty chassis with a 6.0 L V8 gasoline ICE. In addition to these specifications, the other specifications required for modeling the vehicle can be seen in the table below.

Table 2: Specifications used in Simulink model of the GMC Savana 3500 Cutaway Van [20].

Vehicle Specifications	Value	Units
Max Engine Power	324	HP
Max Engine Torque	373	lb-ft
Max Engine Speed	5600	RPM
Rear Axle Ratio	3.73	
Transmission Ratios		
1st	4.03	
2nd	2.36	
3rd	1.53	
4th	1.15	
5th	0.85	
6th	0.67	

The conventional vehicle model was created using SimDriveline components, Simulink Components, and experimental data [18]. In doing so, the vehicle dynamics were modeled using the Vehicle Dynamics block. The transmission was modeled using the Variable Ratio Gear block and the tires using the Simple Tire block. The engine was modeled as a torque source where the torque was interpolated from experimental data based upon the current engine speed and throttle being requested from the controller. To determine the amount of throttle needed, a driver model was created by comparing the drive cycle speed to the simulated speed of the vehicle. This difference was modulated through a Proportional, Integral, and Derivative controller to maintain a speed profile within 2 mph during the entire drive cycle.

HYDRAULIC HYBRID MODEL

In order to model the components which comprise a hydraulic hybrid system, various methodologies were considered and followed. Included in these models were statistical models, experimental data sets, and idealized models. The components which were modeled included high and low pressure accumulators and the hydraulic motors. In addition to these components, the losses occurring due to fluid flowing through the system were also accounted for. Although the addition of the hydraulic technology added numerous components to the model, the following discusses examples of how the individual methodologies were used to model components.

The first task in modeling the hydraulic system involved modeling the thermodynamics of the high and low pressure accumulators. Since hydraulic systems cycle rather rapidly, it is important to capture the thermodynamic response of the nitrogen gas due to compression and expansion. To model this, the Benedict-Webb-Rubin (BWR) Equations of State were modeled

[12]. The BWR equations model the nitrogen filled bladder through the use of experimentally determined and statistically derived coefficients. The BWR equations can be seen below.

$$\frac{dT}{dt} = \frac{T_{amb} - T}{\zeta} - \frac{1}{c_v}\left[\frac{RT}{v}\left(1 + \frac{b}{v^2}\right) + \frac{1}{v^2}\left(B_0 RT + \frac{2C_0}{T^2}\right) - \frac{2c}{v^3 T^2}\left(1 + \frac{\gamma}{v^2}\right)e^{\frac{-\gamma}{v^2}}\right]\frac{dv}{dt} \tag{4}$$

$$P = \frac{RT}{v} + \frac{B_0 RT - A_0 - \frac{C_0}{T^2}}{v^2} + \frac{bRT - a}{v^3} + \frac{a\alpha}{v^6} + \frac{c\left(1 + \frac{\gamma}{v^2}\right)e^{-\frac{\gamma}{v^2}}}{v^3 T^2} \tag{5}$$

$$c_v = \left[\frac{N_1}{T^3} + \frac{N_2}{T^2} + \frac{N_3}{T} + (N_4 - 1) + N_5 T + N_6 T^2 + N_7 T^3 + N_8\left(\frac{N_9}{T}\right)^2 \frac{e^{\frac{N_9}{T}}}{\left(e^{\frac{N_9}{T}} - 1\right)^2}\right] R + \frac{6}{T^3}\left(\frac{C_0}{v} - \frac{c}{\gamma}\right) + \frac{3c}{T^3}\left(\frac{2}{\gamma} + \frac{1}{v^2}\right)e^{-\frac{\gamma}{v^2}} \tag{6}$$

The coefficients used in these equations are statistically determined based upon the gas stored within the bladder of the accumulator. In addition to these values, several other conditions factor into these equations: the ambient temperature, the volumetric change of the nitrogen gas, and the initial conditions of the accumulator. For the purpose of this study, the ambient temperature during testing was set to 70 degrees F. In order to model the heat loss to the environment, the BWR equations incorporate a time constant, ζ, which has been statistically determined for horizontal and vertically oriented accumulators. By definition, ζ is the amount of time which is required for the temperature of the nitrogen gas to decrease 63.2% following a compression cycle. This study will use experimental values obtained through previous studies which have reported a time coefficient of 13.1seconds [13]. The volumetric change of the nitrogen gas bladder was modeled by the displacement of the hydraulic motors. Finally, the initial conditions of the accumulator were determined for precharge of the accumulator and starting pressure. For the purpose of this study, the accumulator was charged to 2500 psi. It was assumed that the accumulator was precharged at standard conditions and that the bladder filled

the total volume of the accumulator. Using the ideal gas law and these conditions, the total molar mass of the nitrogen used for precharging the accumulator could be determined. Using the molar mass of the nitrogen stored within the bladder and the BWR equations, the volume of the bladder could be determined for the starting pressure of the accumulator (3000 psi). These values were then imported into the Simulink model as the initial conditions of the BWR equations. Figure 8 below shows the temperature profile of the accumulator on the HTUF Class 4 Drive Cycle.

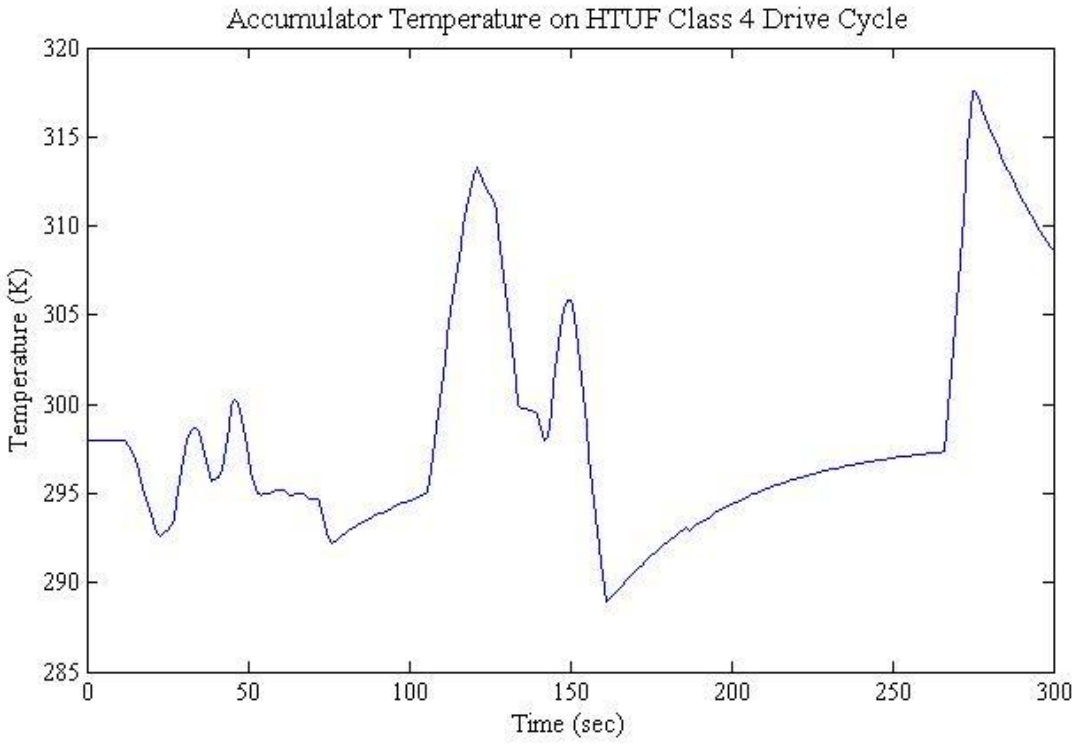

Figure 8: Accumulator Temperature over the first 300 seconds of the HTUF Class 4 Drive Cycle

The hydraulic motors were modeled based upon published efficiency curves using torque sources. The torque available from the motors is a function of a pressure based torque constant and the differential pressure across the inlet and outlet of the motor. When torque is going to be applied to the driveshaft, the efficiency of the motors is determined using the differential pressure. The ideal torque from the motors is multiplied by this efficiency and is then applied to the driveshaft. The plot of the efficiency curves for the hydraulic motors can be seen in Figure 9.

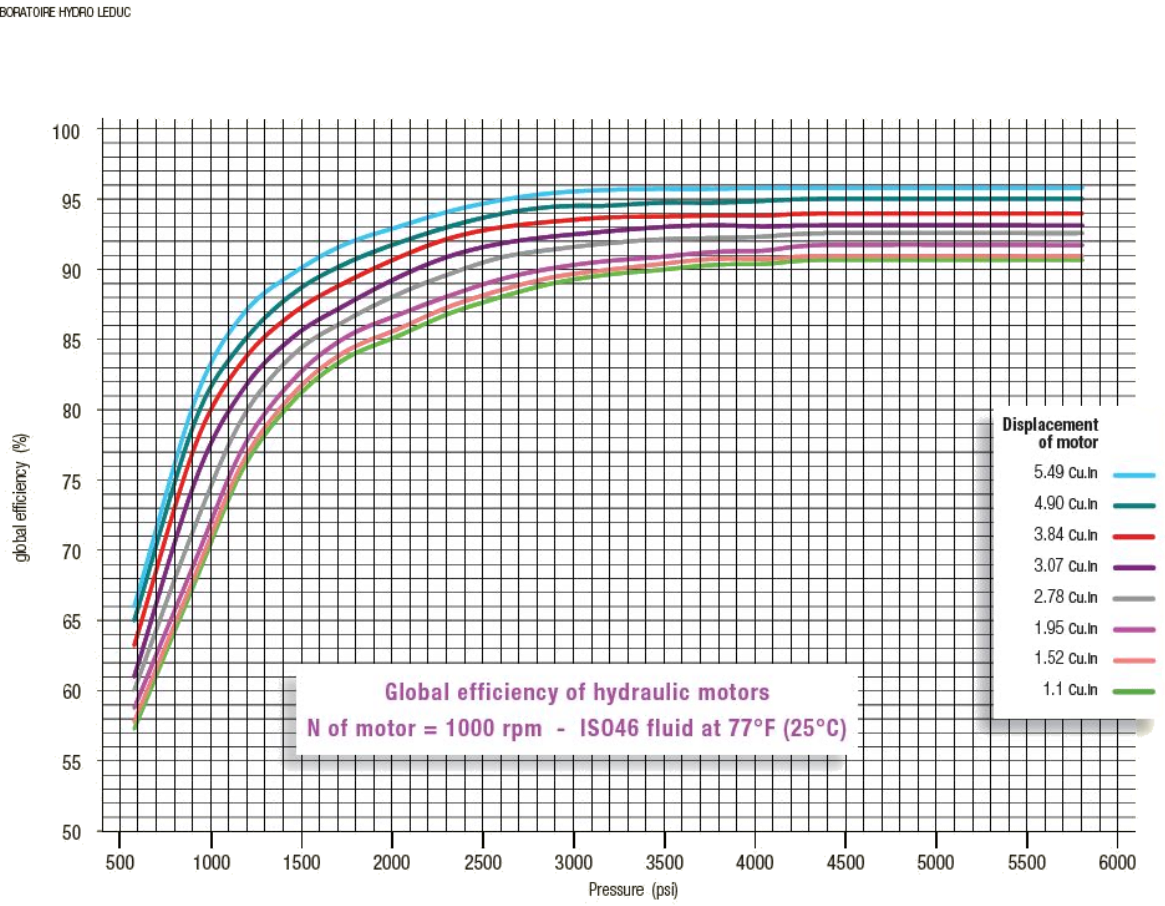

Figure 9: Published Efficiency Curves from the Hydro Leduc MA Series Hydraulic Motors [21]

Data was gathered from the efficiency curves above for each of the available hydraulic motors and was modeled as a lookup table. This table used the differential pressure at the motor inlet and outlet to determine the global efficiency of the hydraulic motors during the simulation.

ELECTRIC HYBRID MODEL

Differing from the lecture notes, the electric hybrid was modeled as a parallel architecture rather than the series architecture which was presented. The only other differing factor between the electric model simulated for this study and the one which was presented in the lecture notes was the method used in modeling the temperature of the battery. The lecture notes presented a constant temperature within the batteries which was used in conjunction with the SOC and a

lookup table to determine the internal resistance of the batteries. Since resistance can be measured within the batteries, the method presented does not account for the heat generated by the internal resistance of the battery. To determine the battery internal resistance, published battery data was modeled as a lookup table based upon the battery temperature and state of charge. This data included a model of a Lithium Ion battery from A123 and a Nickel Metal Hydride. To account for this, it was assumed that all of the power generated by this internal resistance was generated as heat. The following equation shows the instantaneous amount of heat generated by the battery due to the internal resistance.

$$P = I^2 R_{Internal} \tag{7}$$

As can be seen in Equation (7), the heat generated (P) in the battery is a function of the current (I) and the internal resistance ($R_{Internal}$). Given the heat generation as a function of the internal resistance, the change in battery temperature needs to be determined. To determine the change in temperature due to the heat generated, a thermodynamic model was produced to model the heat capacity of the battery as well as model the thermal resistance of the cooling plate contact. This model is shown in the following equation.

$$\dot{q} = \rho C_p V \frac{\partial T}{\partial t} + \frac{\Delta T}{R A_c} \tag{8}$$

The above equation defines the rate at which heat is absorbed ($\dot{q}$) in units of Watts per square meter as a function of the battery heat capacity and the thermal contact resistance [22][23]. The first term defines the change in temperature due to the heat capacity (Cp) of the battery, the density of the battery (ρ), and the volume of the battery (V). The heat capacity of the battery times the density of the battery was determined to be $2.447 \times 10^6\ J/(m^3 K)$ [22]. The second term defines the thermal contact resistance with the cooling plate as a function of the differential temperature (ΔT) and the thermal resistance (R). It was assumed that there was an aluminum to

aluminum contact between the bottom of the battery pack and the cooling plate which provided a thermal resistance of $2.8 \times 10\text{^}(-4)\ \ (K\ m\text{^}2) \ / \ W$ [23]. To determine the amount of heat which the cooling plate absorbed, it was assumed that the contact area between the battery and the cooling plate was 0.07 m^2. The difference between these equations was then combined and multiplied by the internal resistance and contact area. This value was then added to the starting temperature to determine the instantaneous battery temperature. The figure below shows the temperature of an 8.5 Ah battery pack over the HTUF Class 4 Drive Cycle.

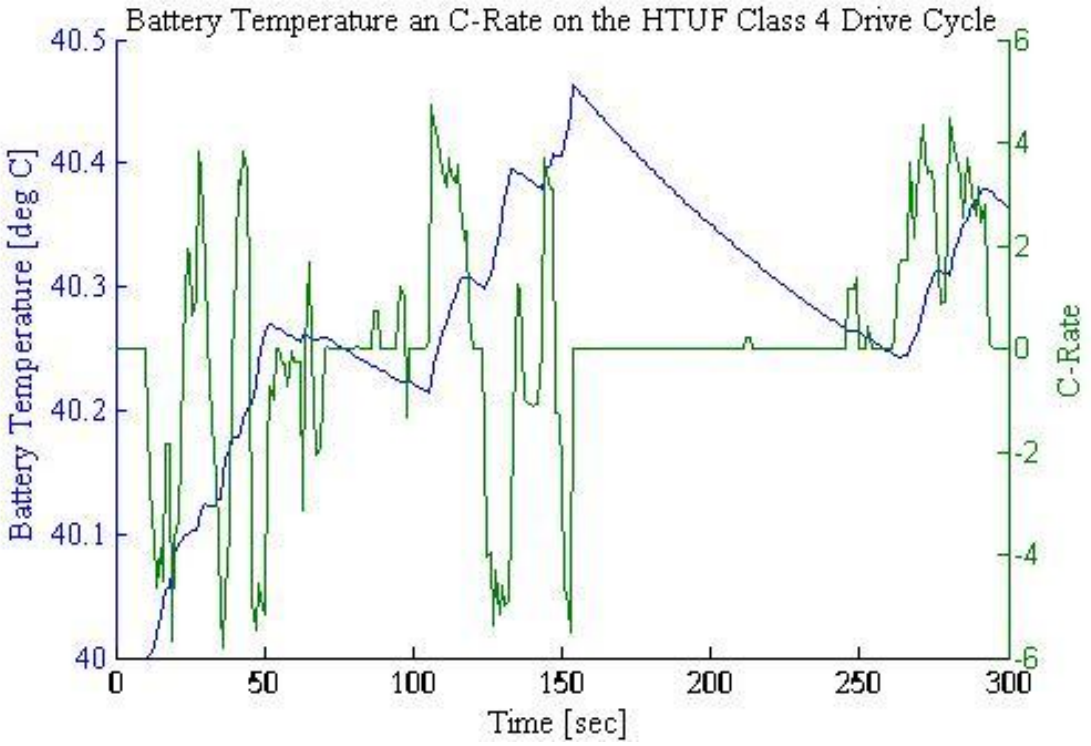

Figure 10: Simulated Battery Temperature over the HTUF Class 4 Drive Cycle

As can be seen in the battery temperature profile over the drive cycle, early on in the drive cycle, the battery is used more due to its SOC and as time progresses, the battery has discharged closer to its minimal limit. Near the minimal limit, the battery usage is much lower which is seen by the lower temperature range at the latter times of the drive cycle. To validate the use of this battery model, two simulations were performed at differing battery temperatures. It was determined that

the difference in fuel economy due to varying battery temperatures (25°C and 45°C) was less than 1%. Due to the small change in fuel economy based on fuel economy, it was determined that this battery model would model the thermodynamics of the battery with enough accuracy that the fuel economy results from the model would not be greatly affected.

MODEL VALIDATION

Each of the vehicle models needed to be validated to verify their utility. In order to validate each model, each model initially needed to be verified against a dynamometer test. Once verified, each model was simulated over a different drive cycle for the same vehicle. This value was then compared to. For the purpose of this study, each model was validated on two parameters. The first parameter is the per mile net tractive energy which is required to complete the drive cycle. The second parameter is the fuel consumed over the same drive cycle.

TRIAL VALIDATION

In addition to using the total tractive energy to validate the simulations, several standards have defined further points of validation for vehicle testing. The first of the standards which will be used to validate the simulations is 40 CFR 86.115-78 – EPA Urban Dynamometer Driving Schedule, which is applicable to all of the models of the vehicle. Second, the Society of Automotive Engineers (SAE) has published the J2711 standards which define the standards for of heavy-duty electric hybrids and dynamometer testing, respectively. Finally, the EPA Smartways Program has proposed testing standards for heavy-duty electric and hydraulic hybrids.

EPA Urban Dynamometer Driving Schedule

The EPA Urban Dynamometer Driving schedule mandates that for a vehicle test to be valid, it must follow the follow the target drive cycle “as closely as possible.” The definition by the EPA for “as closely as possible” is as follows. The vehicle speed must not exceed 2 mph faster or slower than the highest and lowest points of the drive cycle within 1 second of any point of the drive cycle [24].

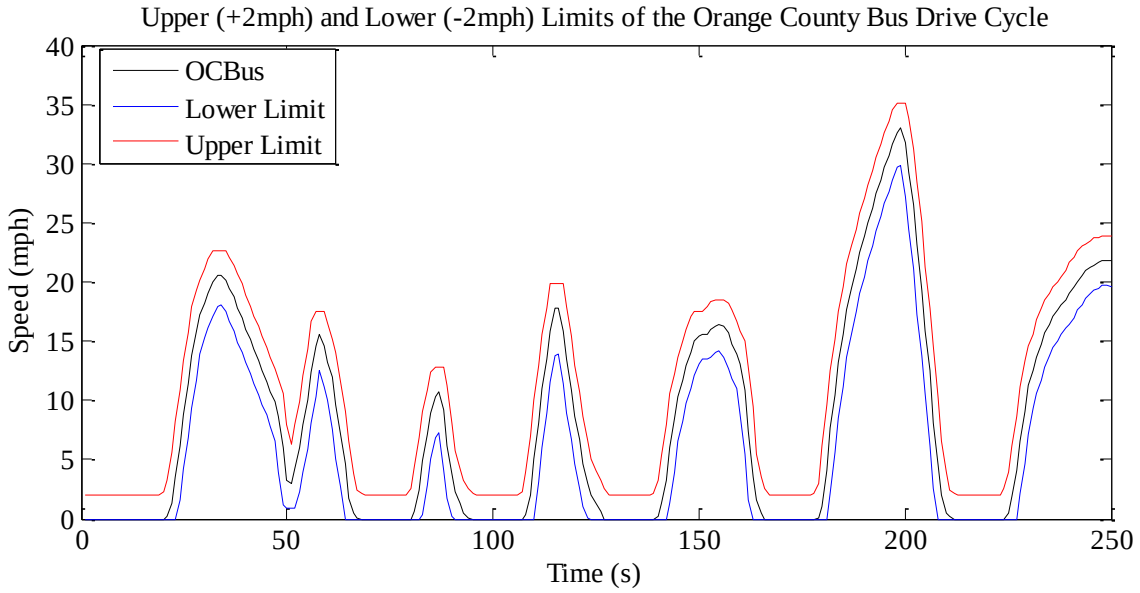

Figure 11: EPA Urban Dynamometer Driving Schedule Validity Limits for the first 250 seconds of the Orange County Bus Drive Cycle

From the above defined standard, a point of validation was made that any vehicle simulation performed which did not meet those guidelines would be deemed invalid.

SAE J2711

To further understand the validation of testing of hybrid vehicles, the standard practices and definitions provided by SAE J2711 were used [25]. J2711 defines the SOC as the actual measured energy content expressed as a percentage of the maximum rated capacity. In addition to defining the SOC for this study, J2711 also provided a correction factor for the SOC. For simulations where a correction to the SOC is required, the following SOC correction method will be used. The method of SOC correction is based upon having several (>3) data points of data that requires correction. With these three points plotted on the basis of change in SOC and fuel economy, a line may be fitted to determine the fuel economy at zero change in SOC. In order for these results to be valid, the line fit must provide a R^2 value no less than 0.8.

EPA Smartways

The EPA Smartways program was created to establish a testing and reporting protocol for heavy-duty vehicles [26]. Within this program, guidelines for establishing valid test has been defined and partially based upon SAE J2711 and the EPA Urban Dynamometer Driving Schedule standard. This program states that for a hybrid test to be valid, as SAE J2711 has previously stated, the change in SOC over a drive cycle must be less than 5%. Within this limit, for a change in state of charge less than 1%, no correction has to be applied. For SOC change between 1% and 5%, a SOC correction factor defined by SAE J2711 must be applied. For hydraulic hybrids, as has been seen previously for electric hybrids, a value of SOC was formed by the EPA Smartways program.

$$SOC = \frac{(144 \cdot P_c \cdot V_c) - \left(144 \cdot P \cdot V_c \cdot \left(\frac{P_c}{V_c}\right)^{1/n}\right)}{1 - n} \tag{9}$$

In Equation (9) above, the SOC for a hydraulic accumulator is a function of the precharge pressure (P_c), the gaseous volume at precharge (V_c), the instantaneous accumulator pressure (P), and the specific heat ratio (n). The EPA provides that for nitrogen gas at high pressures, similar to the operating range of the hydraulic hybrid, the specific heat ratio is 1.8. When solved, it is seen that Equation (9) provides the SOC with units of energy. Therefore, the value for the SOC as it was defined by the EPA Smartways program does not follow the definition of SOC as it was defined by SAE J2711 since it is not a percentage of the total energy storage capacity of the accumulator. In order to better capture the state of charge of the accumulator, the following equation was applied.

$$SOC_{Hydraulic} = \frac{P^{\frac{n-1}{n}} - P_c^{\frac{n-1}{n}}}{P_{max}^{\frac{n-1}{n}} - P_c^{\frac{n-1}{n}}} \tag{10}$$

As can be seen in Equation (10) above, the proposed equation which will be used in determining the SOC for a hydraulic hybrid is a function of the instantaneous pressure (P), the precharge pressure (P_c), the maximum accumulator pressure (P_{max}), and the specific heat ratio (n). The denominator of the equation provides a path to present the value of the SOC as a percentage of the total energy capacity of the accumulator, rather than a value of energy as was seen in Equation (9).

CONVENTIONAL MODEL

To validate the net tractive energy over a drive cycle, data gathered during dynamometer testing will be compared to results from the simulation. The vehicle which was used to validate the model was a GMC Savana 3500 Cutaway Van which had been loaded to a weight of 10,800 lb.

Dynamometer Testing for Model Validation

The dynamometer testing was performed in accordance with the California Air Resources Board Interim Certification Procedures for 2004 and Subsequent Model Hybrid-Electric Vehicles in the Urban and Heavy Duty Vehicle Classes which resulted in the testing of two drive cycles: FTP75 and OCBus which can be seen in Figure 12 [27]. These procedures outline necessary testing requirements for vehicles applying for certifying the use of new medium- and heavy-duty vehicles for operation within the state of California. Prior to the new regulations for Medium- and Heavy-Duty trucks, EPA testing for these classes of vehicles has not been a requirement. Although EPA testing has not been required, CARB has required hybrid system manufacturers to perform this testing, however CARB does not publish this data in its entirety. By having access to dynamometer testing results, data on fuel consumption and tractive energy not otherwise available could be used to validate the conventional and hydraulic models. The net tractive

energy served to validate each configuration against experimental data, and the fuel economy was used as comparative criteria and as a part of the life cycle cost calculation.

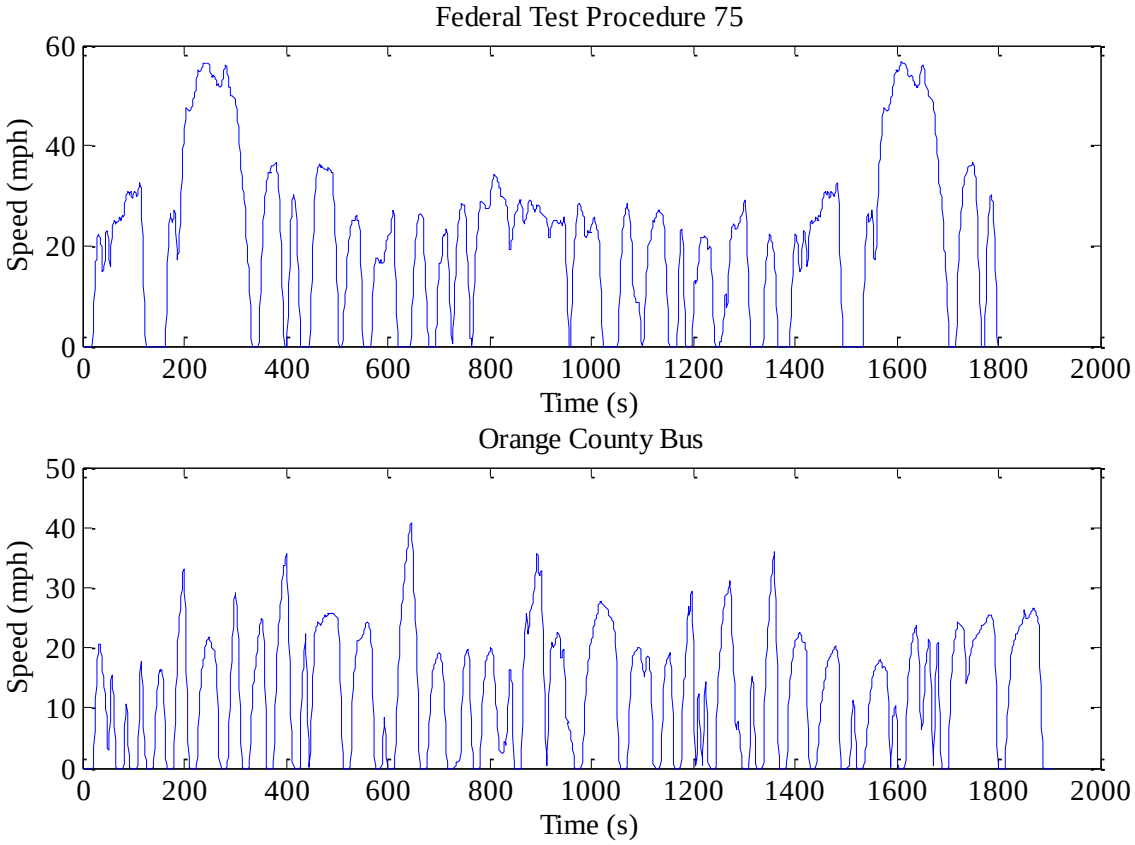

Figure 12: Plots of the Orange County Bus (bottom) and Federal Test Procedure 75 (top) drive cycles

Net Tractive Energy

To calculate the net tractive energy based upon the dynamometer data, the road load equations were used to determine the net tractive energy. These equations use published values for the vehicle and the instantaneous velocity and acceleration from the model. The first equation of this set of equations is for the tractive force and can be seen below.

$$F_{Tractive} = F_{Aero} + F_{Rolling} + F_{Inertia} + F_{Grade} \quad (11)$$

As can be seen in Equation (11) above, the tractive force is a function of the aerodynamic force (F_{Aero}), the rolling resistance force ($F_{Rolling}$), the inertial force ($F_{Inertia}$), and the force due to the

vehicle inclination (F_{Grade}). The OCBus and FTP75 drive cycles used for the validation of and evaluation of the model have no grade change associated with them. Therefore, the F_{Grade} term of Equation (11) above was assumed to be zero. The equations below represent each of the remaining terms in Equation (11).

$$F_{Aero} = \frac{1}{2}\rho\, C_d\, A_f v^2 \tag{12}$$

$$F_{Rolling} = m\, g\, C_{rr} \tag{13}$$

$$F_{Inertia} = m\, a \tag{14}$$

As can be seen in Equation (12) above, the aerodynamic force associated with drag is a function of the air density (ρ), the coefficient of drag (C_d), the frontal area (A_f), and the instantaneous velocity (v) [28]. For this study, the C_d was defined as 0.6 and the frontal area was defined as 9.3 m^2. In Equation (13), the force associated with rolling resistance is a function of the vehicle mass (m), the acceleration due to gravity (g), and the coefficient of rolling resistance (C_{rr}). In order to determine C_{rr}, a coast down test was performed using the Lightning Hybrids LLC GMC Savana 3500 Cutaway. Through this coast down test and the C_d defined above, the C_{rr} was determined to be 0.01774. The inertial force of the vehicle, as seen in Equation (14) above, is a function of the vehicle mass (m) and the instantaneous acceleration (a). The tractive power could then be determined using the tractive force following the equation below.

$$P_{Tractive} = F_{Tractive} * v \tag{15}$$

$$E_{Tractive} = \int P_{Tractive}\, dt \tag{16}$$

In Equation (15) above, the instantaneous tractive power ($P_{Tractive}$) is a function of $F_{Tractive}$ and the instantaneous velocity. By taking the integral of $P_{Tractive}$ over the duration of the cycle, the total cycle tractive energy ($E_{Tractive}$) can be determined as seen in Equation (16). In order to make this data comparable between the dynamometer testing, theoretical testing and simulations, this value

will be divided by the distance which the vehicle traveled over that test and the data will be presented as the net tractive energy. Using the equations defined above, the net tractive energy was determined for the theoretical drive cycle, the dynamometer testing, and the model. The results for this can be seen in the Table 3, below.

Table 3: Net Tractive Energy and Percent Error between Theoretical, Dynamometer, and Simulation Results for the OCBus and FTP75 drive cycles.

	Test	Net Tractive Energy (W/mi)	% Error
FTP75	Theoretical	819.3	-
	Dynamometer	822.8	0.4%
	Simulation	801.3	-2.2%
OCBus	Theoretical	593.7	-
	Dynamometer	597.9	0.7%
	Simulation	566.3	-4.6%

The results of this test show that there is a less than 1% error from the dynamometer testing and the theoretically required net tractive energy. The simulation, however, provides slightly greater change from the theoretical values. Over both simulations, it can be seen that the tractive energy required has a -2.2% change on the FTP-75 Drive Cycle and a -4.6% change on the OCBus Drive Cycle. Given that the allowable 2 mph window in drive cycle testing, the valid window for these drive cycles more than encompasses the error seen in the simulation results. For the FTP-75 Drive Cycle, the 2 mph faster or slower provides a window ranging from -27.8% to 32.7% error from the theoretical value. For the Orange County Bus Drive Cycle, this window ranges from -36.5% to 45.3%. Given the broad ranges provided by the UDDS standard, the Simulations for both FTP-75 and OCBus have verified the model. In addition to verifying the net tractive energy of the conventional and hydraulic hybrid vehicle models, the fuel economy which resulting from the dynamometer and the simulations were compared for the same drive cycles. This comparison can be seen in Table 4.

Table 4: Comparison of Fuel Economies Determined by Dynamometer Testing and Simulations over the FTP-75 and OCBus Drive Cycles

Drive Cycle	Dynamometer Fuel Economy	Simulated Fuel Economy	Percent Difference
FTP-75	11.18	11.15	-0.3%
Orange County Bus	8.31	8.29	-0.3%

In terms of fuel economy, it can be seen in the table above that for both drive cycles, the simulated results are approximately 0.3%. Given the results from this section and the minimal differences seen in both fuel economy and net tractive energy, the conventional model of this vehicle is validated.

HYDRAULIC HYBRID

The hydraulic hybrid was also validated using the same methods as the electric and conventional vehicles. In addition to validating the vehicle dynamics, it was desired to validate the hydraulic hybrid components. To validate the hydraulic hybrid was the net energy change of the high pressure accumulator over the drive cycles. Using the same drive cycles above, the following table provides the net energy change for both dynamometer testing and the simulated results.

Table 5: Comparison of the NEC from Dynamometer Results and Model Simulation of the Hydraulic Hybrid

Drive Cycle	Dynamometer NEC (kW)	Simulated NEC (kW)	Percent Difference
FTP-75	138.8	139.5	0.5%
Orange County Bus	58.0	56.9	-2.0%

When comparing the results for fuel economy from the dynamometer testing to those captured during simulation, it was seen that the error seen was similar to the values seen in the conventional vehicle model. These values can be seen in the following table.

Table 6: Comparison of the Fuel Economy from Dynamometer Results and Model Simulation of the Hydraulic Hybrid

Drive Cycle	Dynamometer Fuel Economy	Simulated Fuel Economy	Percent Difference
FTP-75	12.3	12.2	-0.6%
Orange County Bus	9.1	9.0	-1%

These results show that there is less than 1% difference between the fuel economy recorded during dynamometer testing and that determined from the hydraulic simulations. Given the differences between dynamometer testing and model simulation of the hydraulic hybrid model appears to closely model what was measured on a dynamometer which was used to validate this model.

ELECTRIC HYBRID

To validate the electric model, no dynamometer data was available. To validate the electric model, the Azure Dynamics FedEx GHEV was modeled due to its architecture and gross vehicle weight being similar to that of this study. From a National Renewable Energy Laboratories study, the fuel economy was provided for the Orange County Bus and HTUF Class 4 Parcel Delivery Drive Schedules [31].

Table 7: Comparison of the Fuel Economy from an NREL Field Study and Model Simulation of the Electric Hybrid

Drive Cycle	NREL Fuel Economy	Simulated Fuel Economy	Percent Difference
HTUF-4	11.66 mpg	11.64 mpg	-0.2%
Orange County Bus	8.61 mpg	8.55 mpg	-0.7%

From the results seen in Table 7, the model predicts the fuel economy for the Azure Dynamics HEV as it was studied by NREL within 1% of the tested and published results on the OCBus and HTUF-4 drive cycles. These results verify the models ability to predict the fuel economy for the HEV models.

SIMULATION RESULTS

Using the validated models (Conventional, HEV, and HHV), there simulation cases have been proposed to evaluate the technologies. The first case simulates two similar commercially available systems. The purpose behind this case is to evaluate the current state of the technology available. The second case is for a fixed hybrid system mass. This case will show gains that are obtained and the loss in payload mass for which they come. Finally, the last case which is proposed is for a fixed incremental cost.

HYDRAULIC HYBRID DESIGN

For this study, it was desired to analyze a commercially available system as well as an optimized system. To determine the optimized system, the validated hydraulic hybrid model from the previous chapter was used to study the individual component contribution to the fuel economy benefits. Following this study, a design of experiments will be presented to determine a local optimum for the presented components. The resulting design from this design of experiments will be used for the remaining studies.

To begin the study of component contributions to hydraulic fuel economy improvement, the hydraulic torque source was first to be studied. In a hydraulic hybrid, the amount of torque applied is a result of the maximum system pressure and the size of the pumps. However, the current operating conditions of the system operate at the maximum pressure that some of the main components were designed to which prevents the increase in system pressure as a design variable. This limitation leaves the sizing of the hydraulic pumps as the only possibility for optimizing the torque on the system. In accomplishing this, various pump sizes (Table 8) and combinations were used (Table 9).

Table 8: Hydraulic Pump sizes and properties used to optimize hydraulic torque [21].

Pump Size	Maximum Speed	Maximum Torque
24.9 cc	6300 RPM	164 N-m
32.1 cc	6300 RPM	211 N-m
45.4 cc	5000 RPM	270 N-m

As can be seen in Table 8 above, as the size of the pump increases, the maximum torque also increases. However, this increase in torque comes at the cost of maximum speed of the pumps. With a lower maximum speed, the vehicle would have to brake using its mechanical brakes until the vehicle speed falls within the hydraulic hybrids operational limits and then regenerative braking may begin.

Table 9: Hydraulic Pump combinations used for hybrid system optimization [21].

Pump Combination	Maximum Speed	Maximum Torque	Comb. ID
24.9 cc, 24.9 cc	6300 RPM	328 N-m	1
32.1 cc, 24.9 cc	6300 RPM	370 N-m	2
32cc, 32.1 cc	6300 RPM	422 N-m	3
45.4 cc, 24.9 cc	5000 RPM	434 N-m	4
45.4 cc, 32.1 cc	5000 RPM	481 N-m	5
45.4 cc, 45.4 cc	5000 RPM	540 N-m	6

Table 9, above, shows the maximum possible torques which can be applied by each combination as well as the limitations of the pump combinations. Within the model, the constraints are set as check conditions throughout the model to verify that the components are operating within their published limits. If it is determined that the conditions are outside the published limits, the checks prevent the components from operating until the conditions change. Through using these various pump combinations in addition to a fixed accumulator size, some variation was seen.

Table 10: Improvement of fuel economy for varying pump combinations.

Pump Combination	Fuel Economy Improvement at 4900 kg	Fuel Economy Improvement at 6260 kg
24.9 cc, 24.9 cc	14.7%	25.2%
32.1 cc, 24.9 cc	14.7%	24.6%
45.4 cc, 24.9 cc	14.1%	22.9%
32.1 cc, 32.1 cc	14.8%	23.2%
45.4 cc, 32.1 cc	14.2%	22.5%
45.4 cc, 45.4 cc	14.1%	21.5%

For each of the hydraulic pump combinations, it can be seen that the improvement over stock fuel economy is changed even with constant accumulator size and weight. As the added torque of the pump combinations increase, there is no apparent trend in the fuel economy improvement. It can be seen that there is significant improvement over the stock vehicle in this analysis. This is due to the significantly lower stock fuel economy for this vehicle over the lighter vehicle.

Hydraulic Hybrid Optimization

In order to fully investigate the potential for parallel hydraulic hybrid systems in achieving the model year 2018 goal of the newest fuel economy standards for medium and heavy duty vehicles, a design of experiments was performed to determine the most efficient design of one of these systems. The variables of the design of experiments for the hydraulic hybrid system included pump size (based on currently available pumps), and accumulator volume. In order to investigate the optimum hydraulic hybrid system, a design of experiments was performed for these variables. The hydraulic pumps were varied between the combinations which were defined in Table 9 and the accumulator size was varied between three commercially available sizes. The three accumulator sizes which were simulated included a 37.85 liter, 56.78 liter, and 75.70 liter

accumulator. The fuel economy improvement was recorded for each of the simulations of the design of experiments

The results from the design of experiments described above are shown in Figure 2 below. As can be seen in Figure 3, for each of the pump combinations and accumulator sizes, there is an optimum achievable fuel economy improvement. The pump combinations associated with the numbers in Figure 3 are described in Table 9.

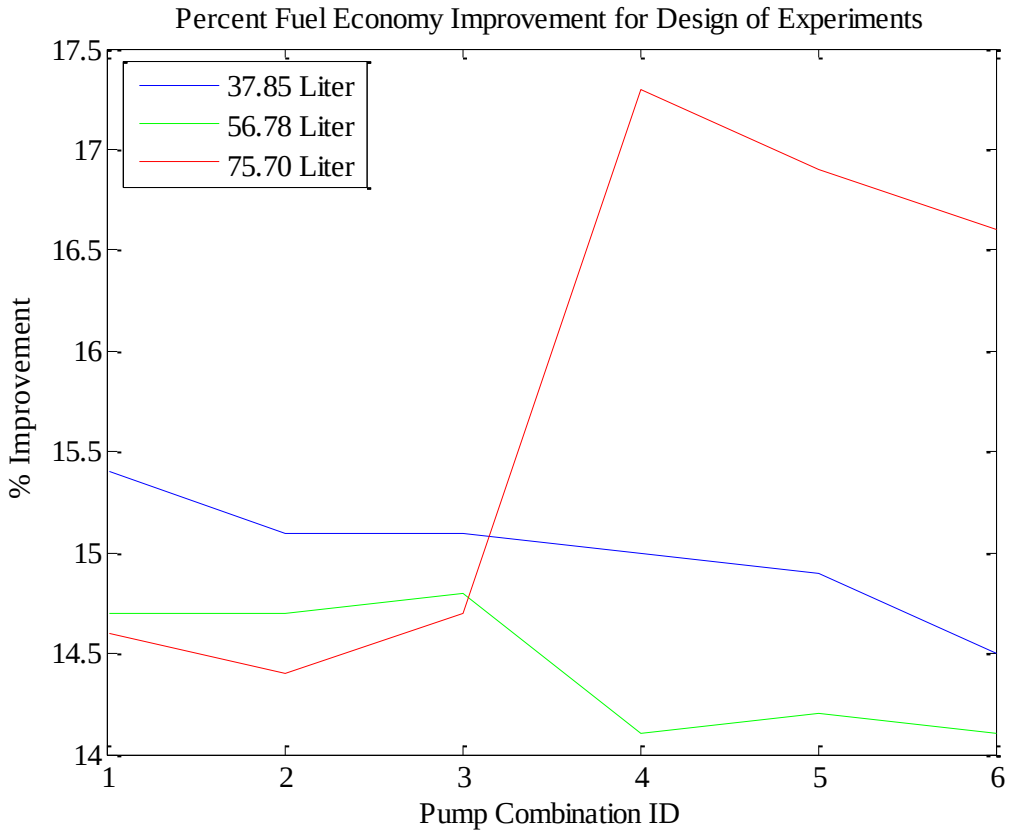

Figure 13: Results of the Design of Experiments

This varying location of the optimum configuration can be explained by the time it takes to brake and accelerate. Due to the nature of the hydraulic pumps, the amount of time taken to fill an accumulator is a function of the pump displacement. Therefore, for each system with a larger combined pump displacement, the optimum accumulator size becomes larger than previous

systems. As can be seen above in Figure 13, the optimum operating configuration for the system contains a 45.4 cc pump, a 24.9 cc pump and a 75.70 liter accumulator. The result, for the drive cycle analyzed, was an improvement of 17% over the stock vehicle.

CASE 1: COMMERCIALLY AVAILABLE SYSTEMS

The first case which was tested was that for commercially available systems. The two systems which were compared consisted of the Azure Dynamics Hybrid Electric and the Lightning Hybrids Hydraulic Hybrid Systems. The table below presents the system configurations for each.

Table 11: Component Configuration for the Azure Dynamics HEV and Lightning Hybrids HHV

	Azure Dynamics HEV [32]	Lightning Hybrids HHV [33]
Hybrid Torque Source	100 kW AC Motor	2x 32cc Fixed Displacement Pumps
Hybrid Energy Storage	288v 8.5Ah Nickel Metal Hydride Battery	15 gallon Bladder Accumulator

Each of the systems was simulated over the 3 drive cycles presented previously in this thesis: HTUF Class 4 Parcel Delivery, Orange County Bus, and Heavy Duty Vehicle UDDS. The table below presents the results of the simulations for both the Lightning Hybrids and the Azure Dynamics Systems.

Table 12: Fuel Economy Results for the Azure Dynamics and Lightning Hybrids Systems

Drive Cycle	Azure Dynamics HEV				Lightning Hybrids HHV			
	Initial SOC	Final SOC	Delta SOC	Fuel Economy	Initial SOC	Final SOC	Delta SOC	Fuel Economy
HDV UDDS	0.8	0.76	0.04	10.50	0.96	0.96	0.00	9.67
	0.85	0.76	0.09	10.45				
	0.75	0.76	-0.01	10.68				
HTUF 4	0.8	0.76	0.04	9.72	0.96	0.98	0.02	9.01
	0.85	0.76	0.09	9.71	0.50	0.97	0.47	9.02
	0.75	0.76	-0.01	9.78	0.79	0.97	0.18	9.01
OC Bus	0.8	0.76	0.04	8.61	0.96	0.96	0.00	9.09
	0.85	0.76	0.09	8.55				
	0.75	0.76	-0.01	8.67				

CASE 2: FIXED HYBRID SYSTEM MASS

The second experiment was designed to determine the improvement in fuel economy based upon a fixed incremental mass. To determine this improvement, the incremental mass due to the hybrid system was fixed at 500 kg. Given this constraint, each of the systems was designed as follows.

The hybrid electric was simulated for 3 designs. The first design was to use a system similar to the Azure Dynamics System and to increase the battery capacity to reach the mass limit of the systems. With the constraint, the battery capacity was increased from 8.5 Ah to 111.11 Ah and the battery power was increased from 60 kW to 100 kW to match the power of the electric motor. The second and third designs were set to increase the motor power in increments of 50 kW and fulfill the remaining hybrid mass envelope through an increase in battery capacity. From this design, it was determined that the second system would have a 150 kW motor and a 103.78 Ah battery and the third system would be composed of a 200 kW motor

and a 96.39 Ah battery. The breakdown of the mass of these electric systems can be seen in the table below.

Table 13: Mass Breakdown for the Hybrid Electric Systems for the Fixed Mass Simulations

	HEV 100 kW	HEV 150 kW	HEV 200 kW	Units
Battery Mass	400.2	373.6	347	Kg
Battery Energy	36.01	29.89	27.76	kWh
Motor Mass	74.8	101.4	128	Kg
Motor Power	100	150	200	kW
Power Electronics Mass	25	25	25	Kg
Total System Mass	**500**	**500**	**500**	Kg

The hydraulic hybrid was designed to meet the design optimization which was discussed as a part of the first research question. As a part of this design, the hydraulic accumulator volume was increased from a 15 gallon, as seen in Case 1, to a 20 gallon accumulator. In addition, the hydraulic motor displacement was changed from two 32cc fixed displacement motors to a combination including a 45.4 cc and a 24.9 cc fixed displacement motor. The simulation results for the above defined hybrid electric and hydraulic hybrid systems can be seen in the table below.

Table 14: Results for the 500 kg system simulations

	HEV 100 kW		**HEV 150 kW**		**HEV 200 kW**		**Optimized HHV**	
Drive Cycle	**Delta SOC**	**Fuel Economy**	**Delta SOC**	**Fuel Economy**	**Delta SOC**	**Fuel Economy**	**Delta SOC**	**Fuel Economy**
HDV UDDS	0.00	10.64	0.02	10.34	0.00	10.67	0.00	9.71
			0.02	10.28				
			-0.001	10.73				
HTUF 4	-0.03	9.46	-0.03	9.57	-0.03	9.66	0.02	9.00
	0.001	9.75	0.001	9.86	0.001	9.91	0.47	9.03
	-0.03	9.53	-0.02	9.63	-0.02	9.72	0.22	9.02
OCBus	0.00	8.64	0.00	8.73	0.00	8.76	0.47	9.18
							0.01	9.11
							0.21	9.14

CASE 3: FIXED INCREMENTAL COST

The final experimental design was to determine the improvement in fuel economy based upon a fixed incremental initial cost. To determine this improvement, the incremental initial cost of the hybrid systems was fixed to $10,900.00. The approach was to design an electric hybrid with as powerful a motor as could possibly fit within the price envelope. The battery was capped at 0.5 Ah which provided enough capital to include a 32.375 kW motor.

Table 15: System Cost Breakdown for the Hybrid Electric Systems in the Fixed Cost Case

	HEV 32.375 kW	**Units**
Battery Cost	$2415.00	
Battery Energy	0.5	kWh
Motor Cost	$8485.00	
Motor Power	32.5	kW
Total System Cost	**$10900.00**	

With the fixed cost system designed, it was then simulated using the criteria drive cycles. The results for these simulations can be seen in the table below.

Table 16: Fuel Economy Results for the Fixed Cost Case

Drive Cycle	**HEV 32.375 kW**	
	Delta SOC	**Fuel Economy**
HDV UDDS	0.06	10.60
	0.01	10.62
	-0.05	10.70
HTUF 4	-0.02	9.71
	0.03	9.74
	-0.07	9.67
OCBus	-0.07	8.56
	0.003	8.57
	0.03	8.60

EVALUATION OF RESULTS

EVALUATION CRITERIA

In order to achieve a real world evaluation of the technologies, the technologies were evaluated for their acceleration performance, fuel economy improvement, and initial system and lifetime costs. The direct result of simulating these technologies with the model is a metric of the acceleration performance and the fuel economy improvement over the specified drive cycles. With this information, the initial and long term costs associated with each technology can be calculated using the fuel economy data and published average cost of ownership equations.

The first of the economic models is the initial cost of the vehicle. The initial cost of the systems is based upon the cost of the chassis and the cost of the components which compose each of the technologies. The tables below show the component costs of each of the technologies.

Table 17: Costs of the individual components used for initial cost determination

Component	**HEV [30]**	**HHV [33]**
Energy Storage	$\$ = 1320 \times E_{Batt} + 1755$	\$1559
Torque Source	$\$ = 262 \times P_{Motor}$	$\$ = 594 \times n_{Pump}$
Clutch	$\$ = 1055 \times n_{Clutch}$	
Misc. Cost		Fluid: 5 $^{\$}/_{quart}$ Manifold: \$4151

As can be seen in the table above, the initial cost for the stock vehicle is made of the chassis and the engine. Additionally, the basis of cost for the electric hybrids varies upon the battery capacity and the rated motor power. Finally, the hydraulic hybrid costs vary around the cost of the accumulator and pump size.

The second of the economic models was that of the life cycle cost of the vehicles. With the initial vehicle cost knowledge, the life cycle cost of the vehicles can be determined. The life

cycle cost of a vehicle is composed of the initial vehicle cost, the cost of fuel over the life of the vehicle, registration, and maintenance. With the fuel economy of each vehicle being produced by the model, the lifetime fuel costs can be determined by using the total miles these vehicles drive during their lifetime. According to the Federal Transit Authority, for medium-duty buses and cutaway chassis (which are used for delivery vehicles), the average life of these vehicles is 7 years and 200,000 miles [29].

INITIAL SYSTEM COST AND MASS

With all of the system designs, the initial system cost and mass of each design was determined based upon component level pricing. Using the component sizes to determine the hybrid system cost, the following table shows the vehicle cost, incremental cost and the mass for each of the hybrid technologies.

Table 18: Vehicle Cost, Incremental System Cost, and Mass for each of the Designed Hybrid Technologies

	Design	Total System Cost	Incremental Cost	System Mass (kg)
Case 1	HEV Azure	$ 59,286.98	$ 30,861.98	163.63
	HHV Lightning	$ 53,425.00	$ 25,000.00	436.36
Case 2	HEV 100 kW	$ 98,316.74	$ 69,891.74	500
	HEV 150 kW	$ 108,607.78	$ 80,182.78	500
	HEV 200 kW	$ 118,898.82	$ 90,473.82	500
	Optimized HHV	$ 53,425.00	$ 25,000.00	500
Case 3	HEV 32.375 kW	$ 38,997.00	$ 10,900.00	96.7

As can be seen in this table, the hydraulic technology provides a pathway where the system level cost is fairly similar between systems. Unlike the hydraulic technology, the electric technology shows a vast range of system costs. The breakdown of component costs for each of the systems can be seen in Appendix II. Additionally, it can be seen that for all instances, with the exception of the fixed mass case, the mass of the hybrid electric systems, is significantly

lower than that of the hydraulic systems. The mass breakdown of each of the vehicles can be seen in Appendix III.

CASE 1: COMMERCIALLY AVAILABLE SYSTEMS

From the simulations of the commercially available hybrid systems, a SOC correction was required for each of the drive cycles and technologies. As was defined earlier in this thesis, the SOC correction is based upon a line fit of 3 or more simulations at varying initial SOC values. From this linear regression, the y axis crossing provides the fuel economy corrected for variation in SOC. The figure below shows the SOC correction for the Azure Dynamics simulation on the HTUF Class 4 Parcel Delivery Drive Schedule.

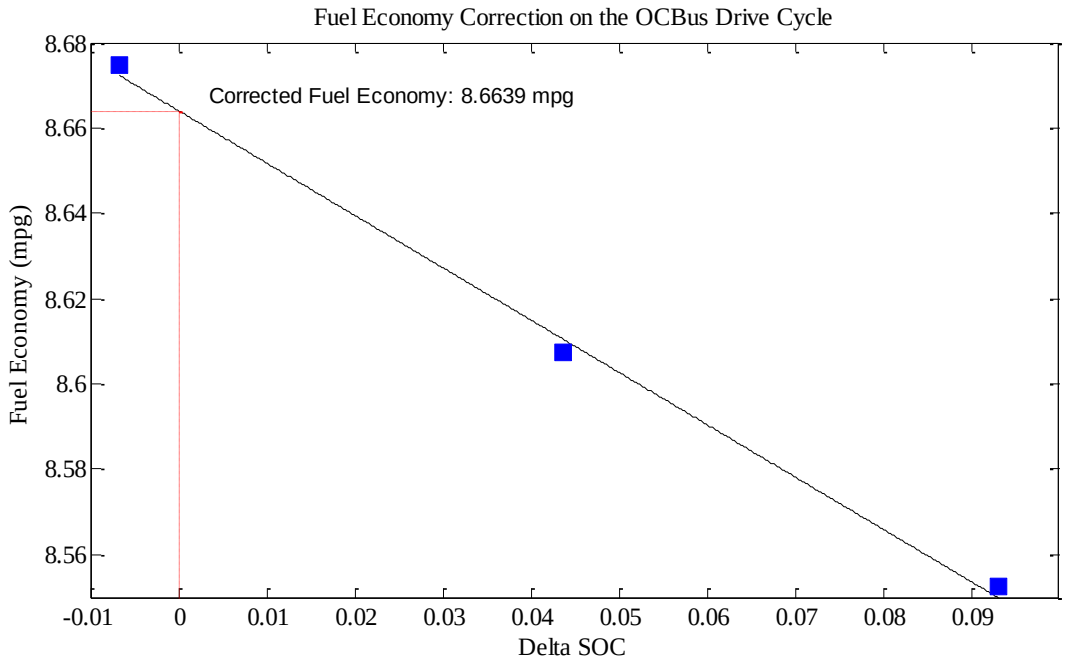

Figure 14: SOC Correction for the Azure Dynamics HEV on the Orange County Bus Drive Cycle

As can be seen in Figure 14 above, the corrected SOC for this simulation was determined to be 9.9249 mpg. This same process was applied to the remaining simulations and the corrected results for this test case can be seen in Figure 14. Using the corrected fuel economy, the life

cycle fuel costs were determined. The following table shows the comparison of the initial cost of each of the systems as well as the total fuel cost over the life of the vehicle accounting for inflation.

Table 19: Corrected Fuel Economy and Incremental and Life Fuel Costs of the Azure Dynamics HEV and Lightning Hybrids HHV Systems

Hybrid System	Incremental Cost	Drive Cycle	Corrected Fuel Economy (mpg)	Lifetime Fuel Cost
Azure Dynamics HEV	$ 30,861.98	HDV UDDS	10.63	$59,628.81
		HTUF 4	9.76	$71,722.05
		OCBus	8.66	$80,795.02
Lightning Hybrids HHV	$ 10,300.00	HDV UDDS	9.67	$72,416.09
		HTUF 5	9.01	$77,700.94
		OCBus	9.09	$77,026.68

As can be seen in Table 19 above, the Azure Dynamics HEV fuel cost steadily increases between drive cycles. The Lightning Hybrids HHV, however, maintains a much smaller distance in fuel costs between each of the drive cycles. Additionally, for these systems, it can be seen that the difference in incremental cost does not affect the outcome of long term cost when compared directly to each other.

CASE 2: FIXED HYBRID SYSTEM MASS

Following the same procedure as above, each of the simulated drive cycle results were corrected using the SAE J2711 procedures where needed. With the corrected drive cycle, the vehicle life fuel cost could be determined. These values, in addition to the incremental cost can be seen in Table 20.

As can be seen in the results for this case, the trends in lifetime fuel costs for each hybrid electric designs (HEV 100 kW, HEV 150 kW, and HEV 200 kW) are similar to each other. For

each of the systems, a difference in lifetime fuel costs for each of the drive cycles varies no more than $800 although there is an increase of approximately $10,300 between each system.

Table 20: Corrected Fuel Economy and Incremental and Life Fuel Costs for the Fixed Hybrid Mass Case

System	Incremental Cost	Drive Cycle	Corrected Fuel Economy (mpg)	Lifetime Fuel Cost
HEV 100 kW	$ 69,891.74	HDV UDDS	10.64	$59,595.18
		HTUF 4	9.75	$71,789.72
		OCBus	8.64	$81,043.84
HEV 150 kW	$ 80,182.78	HDV UDDS	10.70	$59,444.30
		HTUF 5	9.86	$70,677.80
		OCBus	8.73	$79,914.15
HEV 200 kW	$ 90,473.82	HDV UDDS	10.67	$59,227.72
		HTUF 5	9.90	$71,011.92
		OCBus	8.76	$80,162.16
Optimized HHV	$ 10,900.00	HDV UDDS	9.71	$72,116.18
		HTUF 6	9.00	$77,738.91
		OCBus	9.11	$76,849.61

In addition to the trends that can be seen within the electric technologies, it can also be seen that when compared to the electric systems, the hydraulic system, which has a significantly lower initial cost, does not provide as high of a fuel economy as the electrics until the highest kinetic intensity drive cycle, OCBus.

CASE 3: FIXED INCREMENTAL COST

The case of interest within this study was that of fixing the cost of the electric systems to that of the hydraulic ones. These simulations, like the others performed in this study, had the fuel economy results corrected using the SAE J2711 SOC Correction procedures. With the corrected fuel economy, the life cycle fuel costs were determined for the fixed cost design and this can be seen in Table 21, below.

Table 21: Corrected Fuel Economy and Incremental and Life Fuel Costs for the Fixed System Cost Case

System	Incremental Cost	Drive Cycle	Corrected Fuel Economy (mpg)	Lifetime Fuel Cost
HEV 32.375 kW	$ 10,900.00	HDV UDDS	10.34	$61,330.51
		HTUF 4	9.43	$74,245.03
		OCBus	8.36	$83,753.80

For the fixed cost case, a similar trend to the fixed mass case can be seen. For increasing kinetic intensity (HDV UDDS to OCBus), the designs shows a loss in fuel economy. Additionally, the same observations can be made for this case as the previous. When compared to hydraulic hybrid systems, it can be seen that as the kinetic intensity of the drive cycle increases, the electric system and the hydraulic system change places in terms of overall monetary and fuel benefits over the life of the vehicle.

DISCUSSION

Through the evaluation of the simulation results, several key observations pertaining to the hybrid technologies were made.

CURRENT STATE OF THE TECHNOLOGIES

Based on the results from Case 1, some observations can be made pertaining to the current state of the market. This study compared the Azure Dynamics Electric hybrid and the Lightning Hybrids hydraulic hybrid systems. From this study, it was seen that the Azure dynamics provided greater benefits for kinetic intensities less than 3.19.

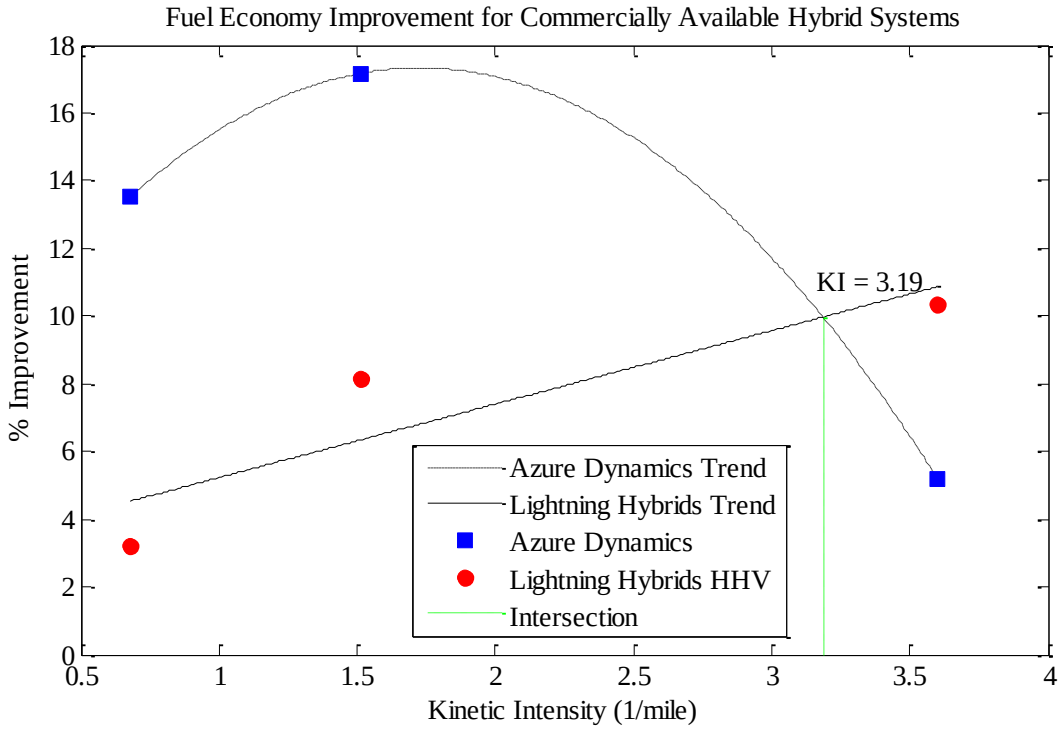

Figure 15: Fuel Economy Improvement for Commercially Available Hybrid Systems in respect to Kinetic Intensity

Although both systems show improvement over the stock vehicle for the drive cycles tested, the costs associated with them is incredibly high. The HEV has an associated incremental cost of $59,287 and a total fuel cost ranging between $59,629 and $80,795. The HHV has an

associated cost of $10,587 and a total fuel cost ranging between $72,116 and $77,701. From the costs associated with each of the technologies, it can be seen that the Lightning Hybrids HHV provides a lower overall cost compared to the comparable Azure Dynamics HEV.

Although the Lightning Hybrids HHV provides a greater economic argument than the Azure Dynamics HEV, the benefit which is seen by these systems does not fully meet the requirements of the new regulations for these classes of vehicles. The Azure Dynamics HEV results in benefits which meet the regulations only for driving conditions with kinetic intensities less than 2.55. Although economics provides backing for the Lightning Hybrids HHV, there are no cases in which the system provides a fuel economy benefit which fulfills the new requirements.

Given the results for these two commercially available systems, it can be seen that within the current state of the market of power-assist hybrid systems, the Azure Dynamics results in the ability to fulfill the new regulations for medium- and heavy-duty vehicles although it comes at a significantly higher cost. The Lightning Hybrids HHV offers a significantly lower cost option in comparison to the HEV, however it only provides partial fulfillment of the requirements. The HHV provides platform which meets the requirements for highly kinetic intense driving for the first 2 years of the adoption of the requirements.

FIXED MASS AND COST SYSTEMS

Through the evaluation of the results from Cases 2 and 3, similar findings can be observed as were for the commercially available systems. The observations made entail the effect of kinetic intensity, the economics associated with each technology, and the ability for each of the technologies to meet the new fuel economy standards.

Effect of Kinetic Intensity

The first of which observation made was the affect of the drive cycles' kinetic intensity on the fuel economy of each system. Through each of the three cases, the same drive cycles, each with a different kinetic intensity from the others, were used to show replicate various uses for the vehicle classes in question. The figure below shows the effect of the fuel economy of each design on the fuel economy.

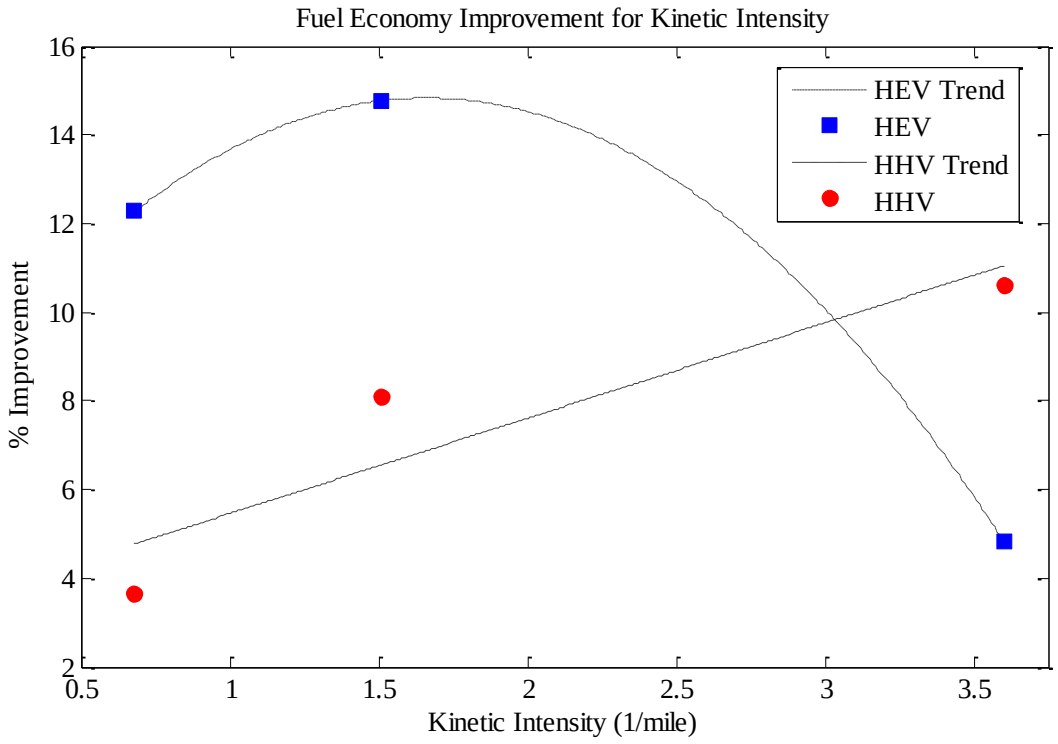

Figure 16: Comparison of the Fuel Economy Improvement of each Hybrid Technology for increasing Kinetic Intensities

From Figure 16 above, the improvement in fuel economy for the HEV designs shows a negative trend with an increase in kinetic intensity, whereas the HHV designs provide for a positive trend in improvement for the same increase in kinetic intensity for the fixed mass case. Given that the general consensus for HEV's and HHV's in these classes of vehicles is that HEV's provide greater savings for lower kinetic intense driving (highway and suburban

deliveries) and HHV's provide greater savings for higher kinetic intense drive cycles (city delivery and bus), the results of this study show that trend in fuel economy improvement agrees with the general consensus. Although the trends seen in the results agree with the general consensus, one individual result does not. The general consensus states that HHV's show a greater improvement for city delivery cycles than HEV's show. In this study, the opposite seems to be true since there was an almost 9% greater fuel economy improvement seen for the HEV's on the HTUF Class 4 drive cycle over the HHV's.

Hybrid Technology Economics

The second characteristic evaluated was the economics of the systems. The economic characteristics which are discussed include the annual fueling costs and the system costs.

To evaluate the annual fueling costs, it is important to analyze the fixed system cost case. This case provides a pathway through which the only variable for the lifetime cost of the vehicle is the annual fueling costs. From the evaluation, it was seen that this Through the evaluation of hybrid electric power assist vehicles with varying motor power and battery capacity, the technology shows lower lifetime fuel costs over the lower kinetic intensity drive cycles than the hydraulic technologies.

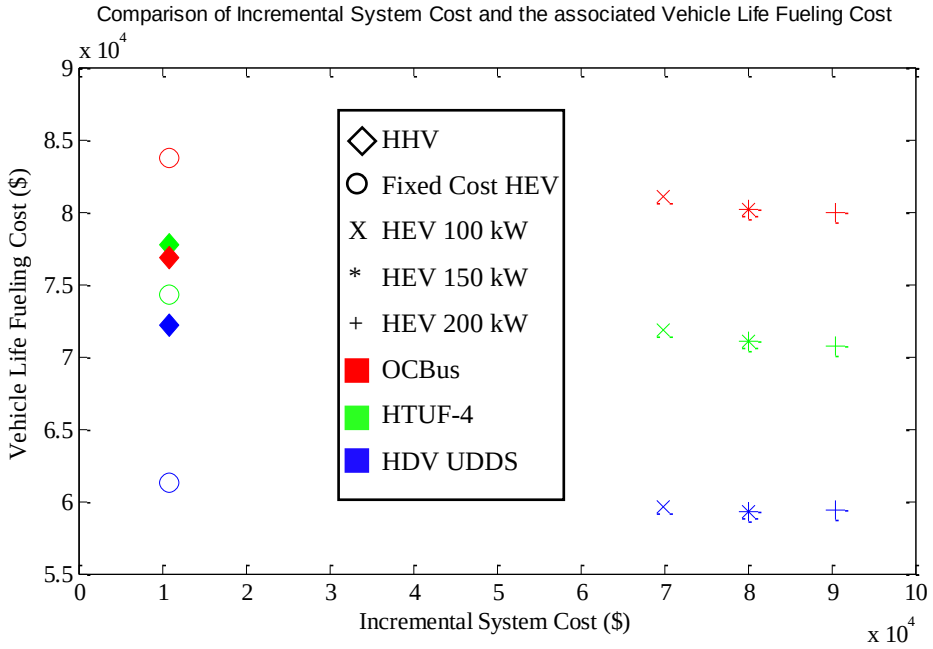

Figure 17: Total Fueling Costs associated with Incremental System Costs

Given the fixed cost results in Figure 17, the range in fueling costs for HEV is greater than that of the HHV. The results for the fixed cost case support the results seen by the kinetic intensity discussion. The HEV technology costs less to operate than the HHV for the case where the system cost was fixed for both systems.

By analyzing the fixed mass systems, it can be seen that there is a negative trend between the system incremental cost and the total fueling costs of the systems. Although the fueling cost decreases with the increase in system cost, the improvement in fueling cost does not make up for the excess system cost.

Through the costs associated with the technologies through either fixing the system mass or the system cost, the HEV technology provides greater savings for driving in cases with kinetic intensities below the OCBus drive cycle. Additionally, on a comparison of systems of fixed cost, it was seen that the HEV provided lower fueling costs than the HHV.

Regulation

The primary reason for analyzing these systems is to fulfill the new fuel economy regulations. Similar to the results seen for the commercially available systems, there are no driving kinetic intensities within the simulated range where the power-assist HHV provides a pathway to fulfill the EPA and NHTSA fuel economy improvements of 15%. The HEV, however, shows improvements which in some cases fulfill the regulations.

CONCLUSION

This study set out to evaluate hybrid electric and hydraulic hybrid technologies for medium and heavy duty vehicles. The basis for this evaluation was to determine the ability for these technologies to fulfill the newly adopted EPA and NHTSA fuel economy regulations for medium and heavy duty vehicles which requires an improvement of 15% by model year 2018. In addition to this evaluation, it was also desired to determine the best technology for a range of kinetic intensities as well as make an economic comparison of the technologies.

To complete these tasks, 3 Matlab Simulink models were created and validated to accurately model the conventional vehicle, and the hydraulic and electric hybrid powertrains. These models were simulated over 3 drive cycles (HDV UDDS, HTUF-4, and OCBus) which covered a broad range of vocations for these vehicles.

From the evaluation of these vehicles, it was seen that a power-assist hydraulic hybrid lacked the capability to fully fulfill the requirements set forth by the EPA and NHTSA. Although the requirements were not fully fulfilled, it was seen that for highly intense drive cycles similar to OCBus, the power-assist hydraulic hybrid provided better fuel economy improvement than the HEV's. Additionally, when compared to an HEV of similar cost, the HHV resulted in fuel savings on the OCBus drive cycle of approximately $7,000 over the life of the vehicle.

Unlike the HHV, the hybrid electric technologies showed a greater improvement on less kinetically intense drive cycles. In addition to this, it was seen that in some cases, the power-assist electric hybrids provided the capability to fulfill the newly established fuel economy requirements under some driving conditions. The one downfall of this technology was the cost associated with it. When compared to an HHV of the same cost, it was seen that for drive cycles

with kinetic intensities less than 2.79 that the HEV was superior to the HHV. However, when compared to the commercially available systems, it was seen that this case was rather ideal. In comparison, the commercially available system cost roughly $20,000 more to produce than the system designed for the fixed cost case.

From the results of this study, it can be concluded that both of these technologies have a place within the market. With new legislation requiring an increase in fuel economy for these vehicle classes, new technology will be required to keep up with the increasing requirements. In addition, the cost associated with each of these technologies has the potential to decrease as production levels increase due to greater demand making these technologies more economically appealing. As has been stated previously, power assist HEV's provide a pathway to fulfill the new fuel economy requirements as the technology stands today. The HHV's however, only partially fulfill the requirements, yet they offer a greater benefit for these vehicles on more kinetically intense drive cycles.

In an attempt to further study the improvements that these technologies could potentially provide these classes of vehicles, future work could study varying architectures (power-split and series architectures) and control strategies (Torque Replacement) to determine the improvement in fuel economy and the associated economics for these technologies as the next step in reducing the fuel usage of these classes of vehicles.

REFERENCES

[1] Robert G Boundy, Stacy C Davis, and Susan W Diegel, "Transportation Energy Data Book,"

[2] Davis, S., Diegel, S., Boundy, R. "Transportation Energy Book Edition 31." ORNL-6987. July 2012.

[3] Environmental Protection Agency, EPA and NHTSA Adopt First-Ever Program to Reduce Greenhouse Gas Emissions and Improve Fuel Efficiency of Medium- and Heavy-Duty Vehicles, August 2011.

[4] The Goodyear Tire & Rubber Company, Radial Truck Tire and Retread Service Manual, 2003.

[5] The National Research Council. Technologies and Approaches to Reducing Fuel Consumption of Medium- and Heavy-Duty Vehicles. Washington D.C. : The National Academies Press, 2010.

[6] Diesel Misers. Diesel Misers Products. [Online] 2012. http://www.dieselmisers.com/Products.htm.

[7] Ehsani, M., Gao, Y., Emadi, A. "Modern Electric, Hybrid Electric, and Fuel Cell Vehicles" Boca Raton, FL. 2010.

[8] Sadeghi, M., Mohammed, A., Rezaii, F. "Hybrid Electric & Hydraulic Drives." LIU-IEI-TEK-A—10/00977—SE.

[9] Mahadevan, R, et al., et al. Battery Technologies. Transportation Technologies for Sustainability. Boulder: Springer, 2013.

[10] U.S. Department of Energy. Batteries for Hybrid and Plug-In Electric Vehicles. Alternative Fuels Data Center. http://www.afdc.energy.gov/vehicles/electric_batteries.html.

[11] Guzzella, L., Sciarretta, A. "Vehicle Propulstion Systems," Springer, Berlin, 2007.

[12] Echter, N. Parallel Hydraulic Pressure Assist/Work Circuit Hybrids for Automated Side Loader Refuse Vehicles. 2012.

[13] Pourmovahed, A., Otis, D. R. (1990), An Experimental Thermal Time-Constant Correlation for Hydraulic Accumulators. ASME Journal of Dynamic Systems, Measurement, and Control. 112.

[14] Analysis of Class 8 truck technologies for their fuel savings and economics. Zhao, Hengbing, Burke, Andrew and Miller, Marshall. August 2013, Transportation Research Part D: Transport and Environment, Vol. 23, pp. 55-63.

[15] Improvement of Citybus Fuel Economy Using a Hydraulic Hybrid Propulsion System - A Theoretical and Experimental Study. Buchwald, P., et al., et al. 1979. SAE Technical Paper 790305, doi: 10.4271/790305.

[16] Hydraulic Hybrid Propulsion for Heavy Vehicles: Combining the Simulation and Engine-In-the-Loop Techniques to Maximize the Fuel Economy and Emission Benefits. Filipi, Z and Kim, Y.J. 1, 2010, Oil & Gas Science and Technology - Rev. IFP, Vol. 65, pp. 155-178.

[17] Lammert, M. Twelve-Month Evaluation of UPS Diesel Hybrid Electric Delivery Vans. National Renewable Energies Laboratory. s.l.: National Renewable Energies Laboratory, 2009. Technical Report. NREL/TP-540-44134.

[18] Hertiner, Marc E. Introduction to Model-Based Systems Design. 2010.

[19] O'Keefe, M.P., Simpson, A., Kelly, K.J. "Duty Cycle Characterization and Evaluation Towards Heavy Hybrid Vehicle Applications." NREL/CP-540-40929. April 2007.

[20] General Motors. 2013 GMC SAVANA CUTAWAY 3500 / 4500 SPECIFICATIONS. GMC.

http://media.gmc.com/content/media/us/en/gmc/vehicles/savana_cutaway_van/2013.tab1.html.
[21] Hydro Leduc N.A., “MA Motor.” www.hydroleduc.com.
[22] Bandhauer, T. M., T. F. Fuller, and S. Garimella. "A Critical Review of Thermal Issues in Lithium-Ion Batteries." Journal of the Electrochemical Society, 158(3): R1-R25. 2011.
[23] Nellis, G., Klein, S. “Heat Transfer.” 2009.
[24] Environmental Protection Agency. “Urban Dynamometer Driving Schedule.” 40 CFR 86.115-78. June 1977.
[25] Society of Automotive Engineers. “Recommended Practice for Measuring Fuel Economy and Emissions of Hybrid-Electric and Conventional Heavy-Duty Vehicles.” SAE J2711. September 2002.
[26] Environmental Protection Agency. “SmartWay Fuel Efficiency Test Protocol for Medium and Heavy Duty Vehicles.” EPA420-P-07-003. November 2007.
[27] California Air Resources Board, "California Interim Certification Procedures for 2004 and Subsequent Model Hybrid-Electric Vehicles in the Urban Bus and Heavy-Duty Vehicle Classes". August 2002.
[28] Kasseris, E.P. “Comparative Analysis of Automobile Powertrain Choices for the Near to Mid-Term Future.” Massachusetts Institute of Technology. June 2006.
[29] Laver, R., Schneck, D., Skorupski, D., et al. “Useful Life of Transit Buses and Vans.” FTA VA-26-7229-07.1 April 2007.
[30] Graham, R. “Comparing the Benefits and Impacts of Hybrid Electric Vehicle Options.” EPRI 1000349. July 2001.
[31] Barnitt, R. “FedEx Express Gasoline Hybrid Electric Delivery Truck Evaluation: 12-Month Report.” NREL/TP-5400-48896. January 2011.
[32] U.S. Department of Energy. “Project Results: Evaluating FedEx Express Hybrid-Electric Delivery Trucks”. DOE/GO-102011-3196. April 2011.
[33] Lightning Hybrids, LLC. www.lightninghybrids.com.

APPENDIX I: BENEDICT-WEBB-RUBIN EQUATIONS OF STATE COEFFICIENTS

Variable	Value	Units
A_0	106.73	$\left(\frac{L}{kg}\right)^2 atm$
B_0	0.04074	$\frac{L}{kg}$
C_0	8.164×10^5	$\left(\frac{L}{kg}\right)^2 K^2\ atm$
a	2.54	$\left(\frac{L}{kg}\right)^3 atm$
b	0.002328	$\left(\frac{L}{kg}\right)^2$
c	7.379×10^4	$\left(\frac{L}{kg}\right)^3 K^2\ atm$
α	1.274×10^{-4}	$\left(\frac{L}{kg}\right)^3$
γ	0.0053	$\left(\frac{L}{kg}\right)^2$
R	0.08206	$\frac{L\ atm}{K}$
N_1	-735.210	K^3
N_2	34.224	K^2
N_3	-0.557648	K
N_4	3.5040	
N_5	-1.7339×10^{-5}	K^{-1}
N_6	1.7465×10^{-8}	K^{-2}
N_7	-3.5689×10^{-12}	K^{-3}
N_8	1.0054	
N_9	3353.4061	K

APPENDIX II: BREAKDOWN OF COMPONENT COSTS FOR EACH HYBRI DESIGN

HEV Cost Breakdown:

	Case 1 Azure Dynamics	Case 2 100 kW	Case 2 150 kW	Case 2 200 kW	Case 3 33.375 kW	Units
Battery Cost	$ 4,986.36	$44,016.12	$41,207.16	$38,398.20	$ 2,415.00	**$**
Battery Energy	2.448	32.016	29.888	27.76	0.5	**kWh**
Motor Cost	$ 26,200.00	$26,200.00	$39,300.00	$52,400.00	$ 8,482.25	**$**
Motor Power	100	100	150	200	32.375	**kW**
Total	**$ 30,861.98**	**$69,891.74**	**$80,182.78**	**$90,473.82**	**$10,897.25**	

HHV Cost Breakdown:

	LHI	Optimized	Units
Accumulator	$ 3,118.00	$ 3,118.00	$
Accumulator Volume	15	20	gallon
Pump	$ 1,188.00	$ 1,188.00	$
Fluid	$ 240.00	$ 320.00	$
Manifold	$ 4,151.00	$ 4,151.00	$
Misc. Cost	$ 2,110.00	$ 2,110.00	$
Total	**$ 10,807.00**	**$ 10,887.00**	

APPENDIX III: BREAKDOWN OF COMPONENT MASSES FOR ELECTRIC HYBRID DESIGNS

	Case 1	Case 2			Case 3	
	Azure Dynamics	100 kW	150 kW	200 kW	33.375 kW	Units
Battery Mass	63.8	400.2	373.6	347	31.9	kg
Battery Energy	2.448	36.01	29.89	27.76	0.5	kWh
Motor Mass	74.8	74.8	101.4	128	38.8	kg
Motor Power	100	100	150	200	32.375	kW
Power Electronics Mass	25	25	25	25	25	kg
Total System Mass	**163.6**	**500**	**500**	**500**	**95.7**	kg

ABBREVIATIONS

AC	Alternating Current
BWR	Benedict Webb Rubin Equations of State
CFR	Code of Federal Regulations
DC	Direct Current
EPA	Environmental Protection Agency
ESS	Energy Storage System
FTP-75	Federal Test Procedure 75
GHEV	Gasoline Hybrid Electric Vehicle
GVW	Gross Vehicle Weight
HDV UDDS	Heavy Duty Vehicle Urban Dynamometer Driving Schedule
HEV	Hybrid Electric Vehicle
HTUF-4	HTUF Class 4 Parcel Delivery Schedule
ICE	Internal Combustion Engine
NHTSA	National Highway and Traffic Safety Administration
NREL	National Renewable Energy Laboratory
OCBus	Orange County Bus Drive Cycle
SAE	Society of Automotive Engineers
SOC	State of Charge
UDDS	Urban Dynamometer Driving Schedule